Arbeitsberichte der Schweizerischen Meteorologischen Zentralanstalt
Rapports de travail de l'Institut Suisse de Météorologie
Rapporti di lavoro dell'Istituto Svizzero di Meteorologia
Working Reports of the Swiss Meteorological Institute

Zürich

52705

No 134

QUALITY CONTROL OF THE SWISS NETWORK RADIATION DATA

by

Alain Heimo, Zurich

December 1985

Automatic station	551.508.824
Solar radiation	551.521.1
Instrument control	53. 089.6

Summary

The automatic network ANETZ of the Swiss Meteorological Institute is equipped for radiation measurements. The necessary quality control of the gathered data implies the use of redundant information which is available at the World Radiation Center in Davos where reference instruments are installed together with a prototype device for the measurement of the direct irradiance.

Quality controls of the 10 minute interval measurements are performed successively for sunshine duration, global horizontal irradiance, direct irradiance and luminosity. Though some teething problems still exist, the general quality of the studied material may be considered as satisfactory over the two year test period. Suggestions for further developments of the network are presented throughout the study.

Resumé

Le réseau automatique ANETZ de l'Institut Suisse de Météorologie inclut des mesures de rayonnement. Le contrôle nécessaire de la qualité des données implique l'utilisation d'informations redondantes qui sont à disposition au Centre Mondial du Rayonnement à Davos où sont installés des instruments de référence ainsi qu'un système prototype de mesure de l'irradiance directe.

Un contrôle de qualité des mesures effectuées sur des intervalles de dix minutes est présenté pour la durée d'ensoleillement, l'irradiance globale horizontale, l'irradiance directe et la luminosité. Bien que certains problèmes d'enfance aient été décelés, la qualité générale du matériel étudié peut être considérée comme satisfaisante pour la période test choisie de deux années. Des suggestions quant à de futurs développements du réseau sont présentées tout au long de l'étude.

Riassunto

La rete automatica ANETZ dell'Instituto Svizzero di Meteorologia effettua misure dell'irraggiamento. Il necessario controllo della qualità dei dati implica l'uso di informazioni supplementari, disponibili al Centro Mondiale per l'Irraggiamento di Davos, presso il quale sono installati strumenti di riferimento oltre ad un prototipo per la misura dell'irraggiamento diretto.

Controlli di qualità delle misure effettuate a intervalli di 10 minuti sono stati fatti per la durata dell'insolazione, l'irragiamento globale orizzontale, l'irraggiamento diretto e la luminosità. Nonostante vi siano ancora alcuni problemi, la qualità del materiale studiato è da considerare, in generale, soddisfacente per il periodo scelto di due anni. Suggerimenti per il futuro sviluppo della rete vengono presentati nel corso dello studio.

Zusammenfassung

Das automatische Messnetz der Schweizerische Meteorologischen Anstalt (ANETZ) ist ausgerüstet für Strahlungsmessungen. Die notwendige Qualitätskontrolle der Daten erfordert die Benützung von redundanten Informationen die am Weltstrahlungszentrum in Davos vorhanden sind. Dort sind Referenz-Instrumente und ein Prototyp-Messsystem für die Messung der direkten Einstrahlung installiert.

Die Qualitätskontrolle der Messungen in einem 10 Minuten Intervall wird für die Sonnenscheindauer, die globale horizontale Einstrahlung, die direkte Einstrahlung und die Helligkeit dargestellt. Obwohl noch einige kleinere Probleme vorhanden sind, darf die Qualität des untersuchten Materials für die gewählte zweijährige Testdauer als befriedigend betrachtet werden. Empfehlungen für spätere Entwicklungen werden laufend in der Untersuchung vorgebracht.

Table of contents

	Pages
1. Introduction	1
2. Sunshine duration	4
3. Global radiation	11
4. Direct radiation	17
5. Luminosity	35
6. Conclusions	54
7. Acknowledgements/References	56

Abbreviations

ANETZ	: Automatic network of the Swiss Meteorological Institute.
WRCD	: World Radiation Center, Davos.
RASTA	: Radiometer for the automatic station.
SODA	: Sunshine duration.
GHA	: Global irradiance for a horizontal surface recorded by the ANETZ pyranometer CM6.
GHD	: Global irradiance for a horizontal surface recorded by the WRCD pyranometer PSP.
DHD	: Diffuse irradiance for a horizontal surface recorded by the WRCD pyranometer PSP.

1. INTRODUCTION

During the past ten years, the Swiss Meteorological Institute has developed an automatic network called ANETZ (Automatisches NETZ) to measure most of the meteorological parameters normally required. More than 60 stations distributed over the whole country are currently in operation. The mean spatial coverage is one station for 680 km^2, corresponding to a mean grid with edges of 26 km. Altitudes range from 197 to 3580 m.a.s.l.. The ANETZ is probably one of the densest networks in the world; the numerous types of climatic conditions which are recorded can be considered as representing a unique tool for research as well as for climatological and meteorological purposes, but they are also the source of many difficulties when comparisons between the stations are requested.

Each station is equipped with a sunshine recorder device SOLARIMETER SOLAR 111 from Haenni. It is mounted in a free environment, oriented towards south and its axis is tilted as function of the latitude of the station. Six internal solar cells are continuously recording the solar radiation. A rotating screen passes in front of the cells and masks out the direct radiation whenever present, yielding a pulse which is used to determine the occurence of sunshine. The intensity threshold level can be adjusted to 200 W/m^2, a WMO recommended value.

Apart from the sunshine duration, each station records the global horizontal irradiance with a ventilated Kipp & Zonen CM6 PYRANOMETER. The output voltage is digitalized and continuously integrated. The offset is determined by averaging the values between 0:00 and 3:00 UT and the counter is reset to zero at 0:00 UT.

The last routine radiation instrument is a luminosity recorder. It is a simple photodiode covered by a hemispheric glass dome. Its spectral absorption curve is not adapted to the human eye by the spectral luminous efficiency function $V(\lambda)$ and, therefore, it cannot be considered as a real lux-meter. However, calibrations performed with a reference instrument showed a good correlation and an approximately cosine square directional response. This means that the photometric information has its maximum weight at the zenith luminosity.

Cyclic maintenance of the network is performed regularly and includes controls of the instruments by calibration transfer at least once every two years.

The signals of all radiation instruments are continuously integrated over one day. The content of the counters are stored in the local memory every 10 minutes. These values are called by the central station within the next 10 minute period through the telephon network. Conversion into physical units according to the individual characteristics of each instrument is then performed, allowing a first quality control of the data at this stage: whenever difficulties are encountered, appropriate actions are then undertaken.

From the very beginning of the development of the network, it was evident that the measured radiation parameters were necessary but not sufficient to gather a full view of the radiative processes taking place. More specifically, the need for information about the direct and diffuse components of the solar irradiance was voiced by different scientific groups interested in either atmospheric physics or engineering, in the latter case mostly for solar energy and building applications. As redundancy could not be afforded, only one of those parameters had to be measured while computing the missing information. Switzerland enjoys the presence of the highly competent WRCD in this field and, since this institute had developed very accurate active cavity absolute radiometers, the choice for the measurements of the direct component was made.

The problem was certainly not trivial: the new system had to be operated in a routine network, with only sporadic maintenance. The new product was a fully automatic, microprocessor driven, passive sun-tracker supporting a specially adapted ventilated absolute radiometer PMO6 and received the name RASTA (Radiometer for the Automatic STAtion). A first prototype was put in operation on the 1st of January 1982 in Davos where one of the automatic stations is running.

In order to gather more experiences with this new, relatively complex equipment, the construction of further units was delayed until a quality test over a long period could be performed. For that purpose, measurements of the global and diffuse horizontal irradiances with WRCD instruments were used. A series of preliminary tests was

conducted in February 1982 during an 18 day test period. The results are presented in (1). One of the goals of the present project is to study the behaviour of the RASTA system during the first two years of operation.

Another consequence due to the installation of the RASTA system together with reference instruments in Davos, lies in the possibility to test the other radiation instruments with the available redundancy:

- sunshine duration with the RASTA direct irradiance,
- luminosity with the global irradiance, at least for the diurnal part of the day,
- global irradiance with 2 different instruments,
- direct irradiance from the global and diffuse horizontal irradiances.

This is a unique possibility to investigate the general behaviour and quality of the available radiation parameters over a longer period.

The aim of this work is to determine, as far as possible, the quality of the routine instruments of the network. The validation of the RASTA will be undertaken and an attempt to make use of the luminosity measurements at day and at night will be described. Further developments will be suggested in the conlusion.

2. SUNSHINE DURATION

Sunshine duration is a widely used parameter either directly for meteorological and climatological purposes or as input for the modelling of other radiative components and climatological data needed for example in the building industry.

The data collected by the ANETZ are digitalized in the number of minutes per 10 minute intervals where the direct irradiance is above the threshod of 200 W/m^2: thus the values range from 0 (no-sun) to 10 (full-sun) minutes (figure 2.1). Table 2.1 shows the monthly distribution of the different cases over a 19 month period. It is interesting that the measurements out of range (column "RANGE") are non-existent. Untransmitted data are more frequent, though not in a drastic way (column "TRANS"): as the system integrates continuously over the day, this effect becomes negligible when considering hourly values, since single transmission errors are relevant only for the last interval before an hourly counter reading.

Another interesting aspect from the climatological point of view is the dominant weight of the no-sun (s=0) and full-sun (s=10) cases in comparison with the intermediate situations ($1 <= s <= 9$).

In order to study the quality of the recorded sunshine duration values, the assessment of the good behaviour of the RASTA system is made. It is then justified to investigate if

1. for the cases where s = 10, the irradiance values are above the threshold limit,
2. for the cases where s = 0, the irradiance values stayed below the threshold level.

No particular problem was found concerning the first test. But figure 2.2 shows the percentage of cases where no sun was recorded by the sunshine recorder while the direct irradiance intensity exceeded 200 W/m^2. It is evident that we are facing here a problem: during the summer 1982, up to 30% of the cases per month showed this strange behaviour. The results look somehow better in the next winter, but start to degrade again in the summer 1983. After August 1983,

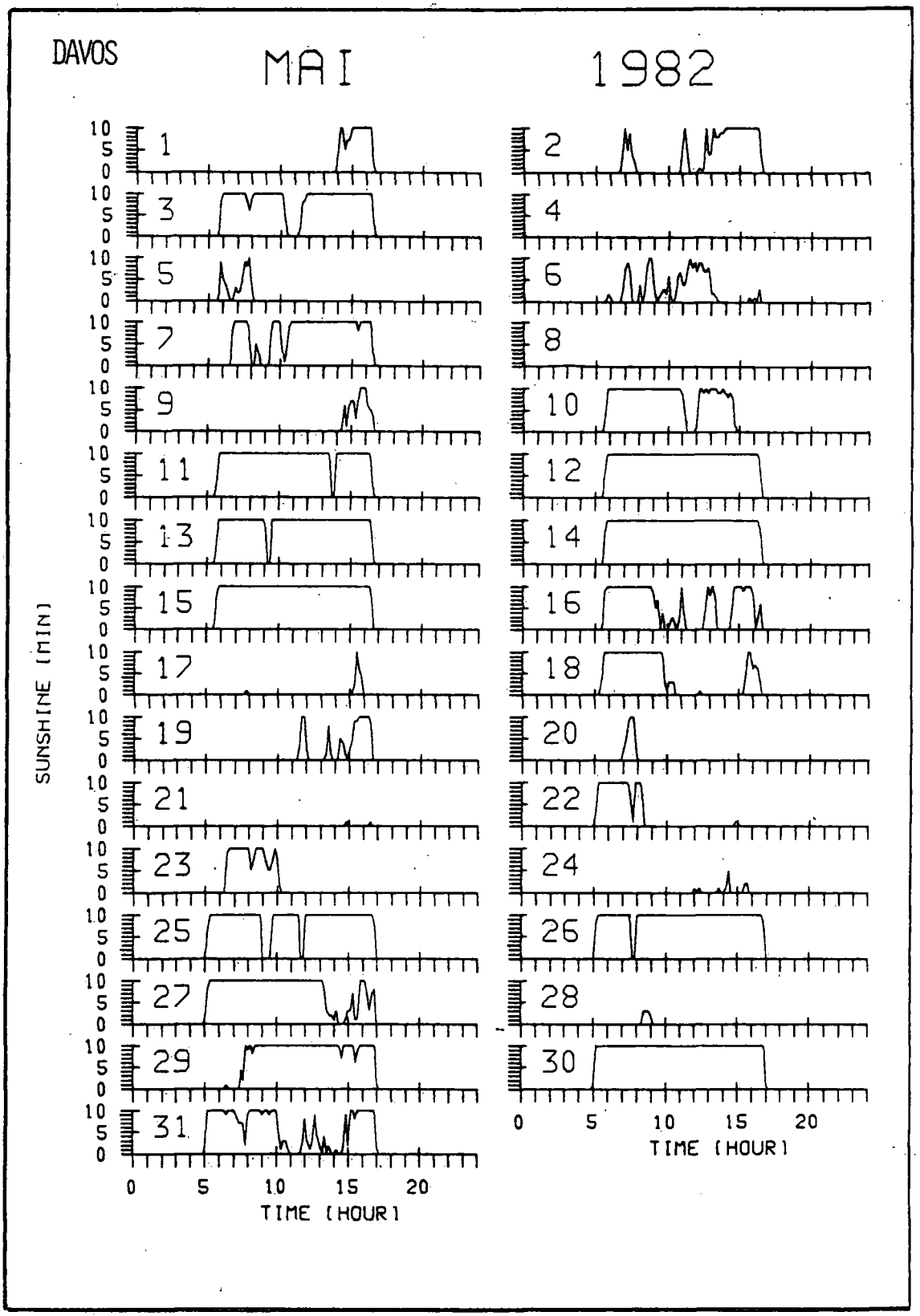

Fig. 2.1 Daily variation of the sunshine duration for 10 minute intervals. The number of the day is written on the upper left part of each diagram.

SUNSHINE DURATION : FREQUENCY TABLE

STATION : DAVOS

MONTH	YEAR	TOT	S=0	S=1	S=2	S=3	S=4	S=5	S=6	S=7	S=8	S=9	S=10	TRANS	RANGE
JANUARY	1982	1640	1064	11	14	8	12	10	5	6	8	16	450	36	0
FEBRUARY	1982	1699	800	20	13	13	11	13	11	14	11	20	680	53	0
MARCH	1982	2180	1253	47	31	27	23	19	25	23	29	50	626	27	0
APRIL	1982	2413	1350	50	37	34	34	24	31	36	20	36	712	49	0
MAI	1982	2758	1543	39	33	35	25	21	16	29	30	35	914	33	0
JUNE	1982	2809	1805	68	50	42	39	25	35	30	45	57	539	74	0
JULY	1982	2834	1524	66	48	45	41	60	39	56	52	66	789	48	0
AUGUST	1982	2601	1613	56	29	32	25	26	19	38	36	61	632	34	0
SEPTEMBER	1982	2230	942	37	40	21	29	29	20	25	20	45	959	63	0
OCTOBER	1982	1993	1038	32	22	18	21	17	21	16	18	23	670	97	0
NOVEMBER	1982	1656	926	30	24	17	18	17	12	17	20	19	530	26	0
DECEMBER	1982	1569	933	28	27	23	21	18	24	20	14	26	420	15	0
JANUARY	1983	1638	1011	21	16	12	8	14	11	12	15	15	500	3	0
FEBRUARY	1983	1697	830	20	18	6	12	6	5	13	14	15	742	16	0
MARCH	1983	2179	1280	18	18	15	9	18	12	17	11	16	738	27	0
APRIL	1983	2410	1794	48	33	31	30	35	27	21	23	31	326	11	0
MAI	1983	2757	2135	49	36	27	18	16	19	21	27	40	307	62	0
JUNE	1983	2808	1831	68	37	37	36	30	25	25	39	55	594	31	0
JULY	1983	2834	1253	66	47	39	49	49	62	49	46	88	1069	17	0
AUGUST	1983	2602	1520	66	43	37	40	35	33	31	43	52	682	20	0
SEPTEMBER	1983	2232	983	68	40	38	22	24	36	36	40	55	828	62	0
OCTOBER	1983	1994	836	17	20	21	32	12	17	16	11	21	966	25	0
NOVEMBER	1983	1658	713	18	11	3	7	7	13	8	10	15	827	26	0
DECEMBER	1983	1570	839	17	21	15	10	12	14	16	12	16	594	4	0
TOTAL		52761	29816	960	708	596	572	537	532	575	594	873	16094	904	0

Table 2.1 Monthly frequency table of the sunshine duration for the test period.

TOT: : Total number of cases where the sun's elevation is higher than 0 degree.

S : number of minutes of sunshine per 10 minute interval.

TRANS: number of transmission errors.

RANGE: number of cases where the sunshine duration values are outside boundaries.

the problem seems to disappear. Snow is therefore NOT responsible for such an effect: this assumption was often made since Davos lies in a valley surrounded by high mountains constantly covered by snow during the winter months.

In order to understand under which special conditions the errors seem to happen, the distribution of the diffuse (figure 2.3), global (figure 2.4) and direct (figure 2.5) irradiances for the dubious cases has been investigated: 18.5% of the readings are considered as faulty over the whole test period. Most of these errors occur for diffuse irradiance values between 300 and 500 W/m^2, i.e. for rather

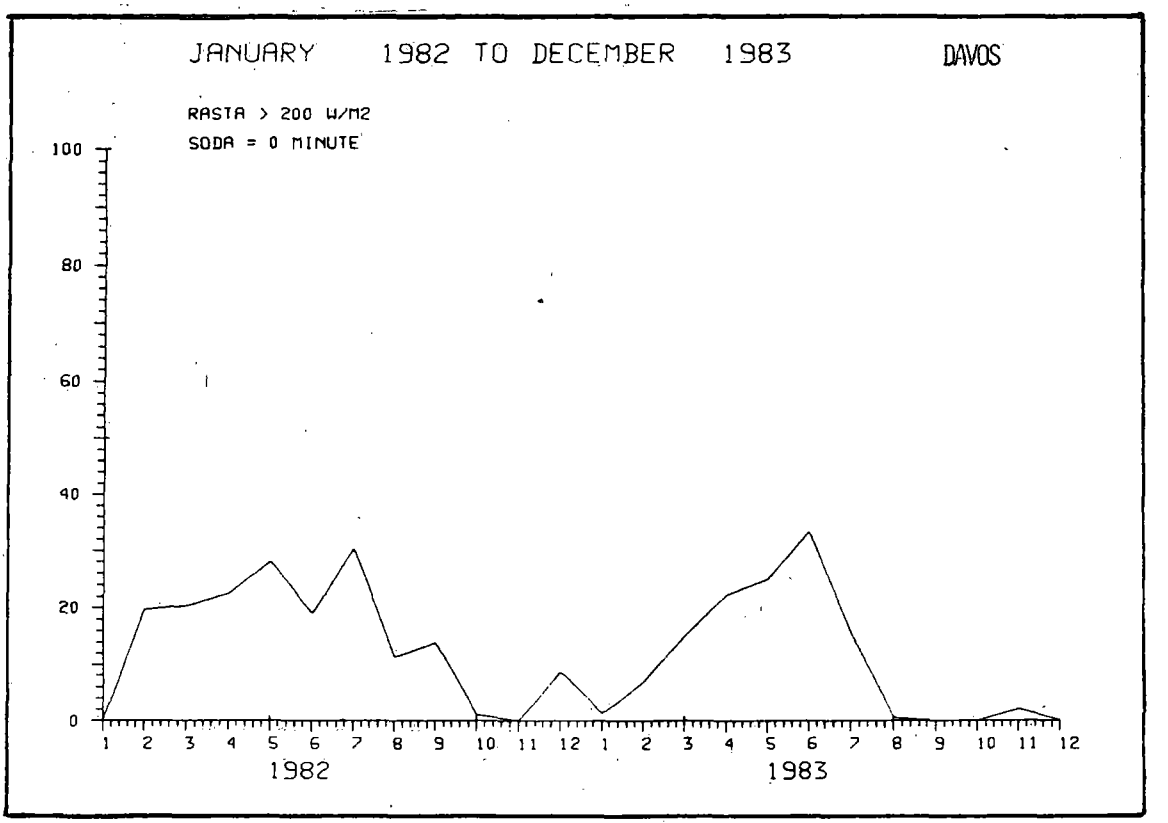

Fig. 2.2 Monthly relative distribution of the cases where the sunshine duration was equal to 0 while the direct irradiance intensity was superior to 200 W/m^2.

high global and low direct intensities. This suggests that the failures are taking place for highly diffuse situations, when the sun is shining, i.e. in the presence of thin clouds. Davos is a network station where cloud observations are performed 3 times a day. This information is accessible and the distribution of the cloud cover for the concerned cases is presented in figure 2.6. The full line displays the cloud cover expressed in octas and the scale is extended to 9 for transmission errors. The broken line represents the opacity or thickness of the clouds. Its scale goes from 0 to 2, 0 being the cloud free state and 2 being equivalent to very thick clouds. It is evident from the graph that the dubious cases are appearing for medium to high cloud cover and for rather bright clouds. This kind of meteorological conditions are met in mountain in summer because of the buildup of convective clouds on the tops of the surrounding summits, explaining therefore the annual variation presented in figure 2.2.

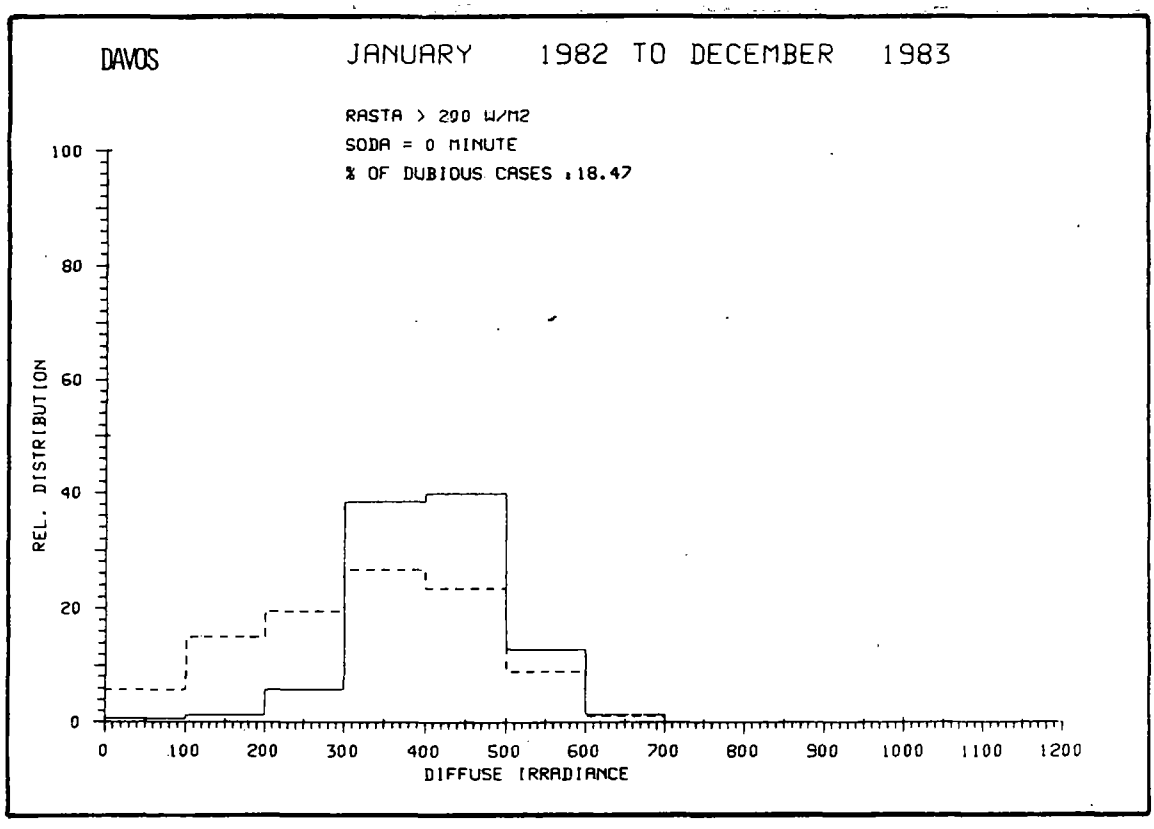

Fig. 2.3 Relative distribution of the sunshine duration dubious cases as function of the measured diffuse irradiance (full line). The broken line indicates the relative distribution of the reference irradiance for the whole set of points without sunshine.

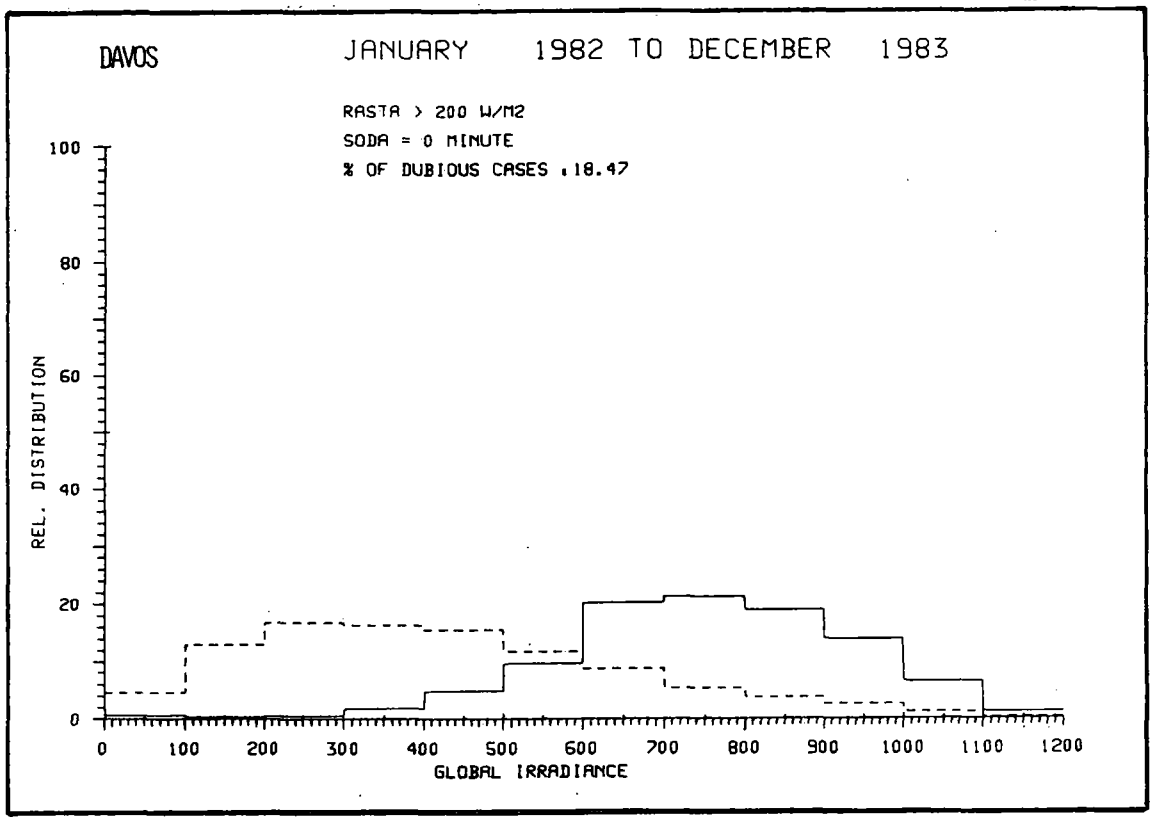

Fig. 2.4 Same as fig. 2.3 with the global irradiance taken as reference.

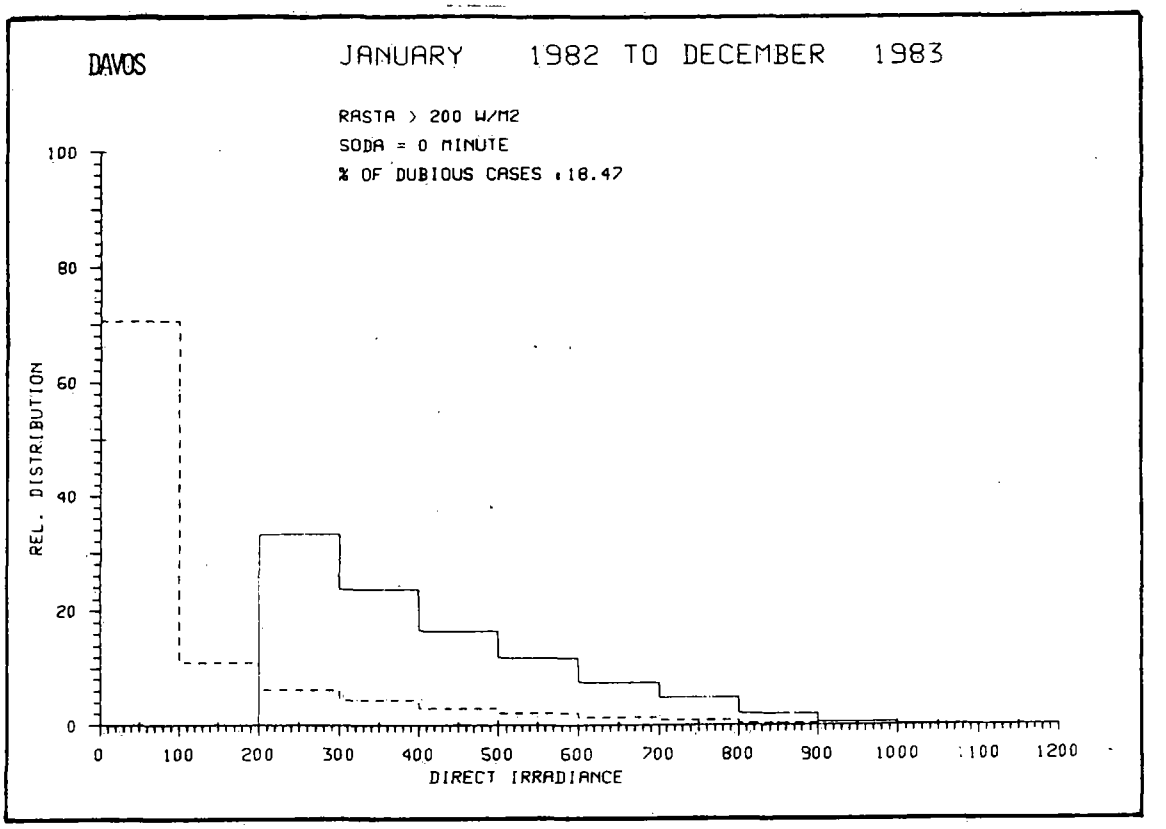

Fig. 2.5 Same as Fig. 2.3. with the direct irradiance taken as reference.

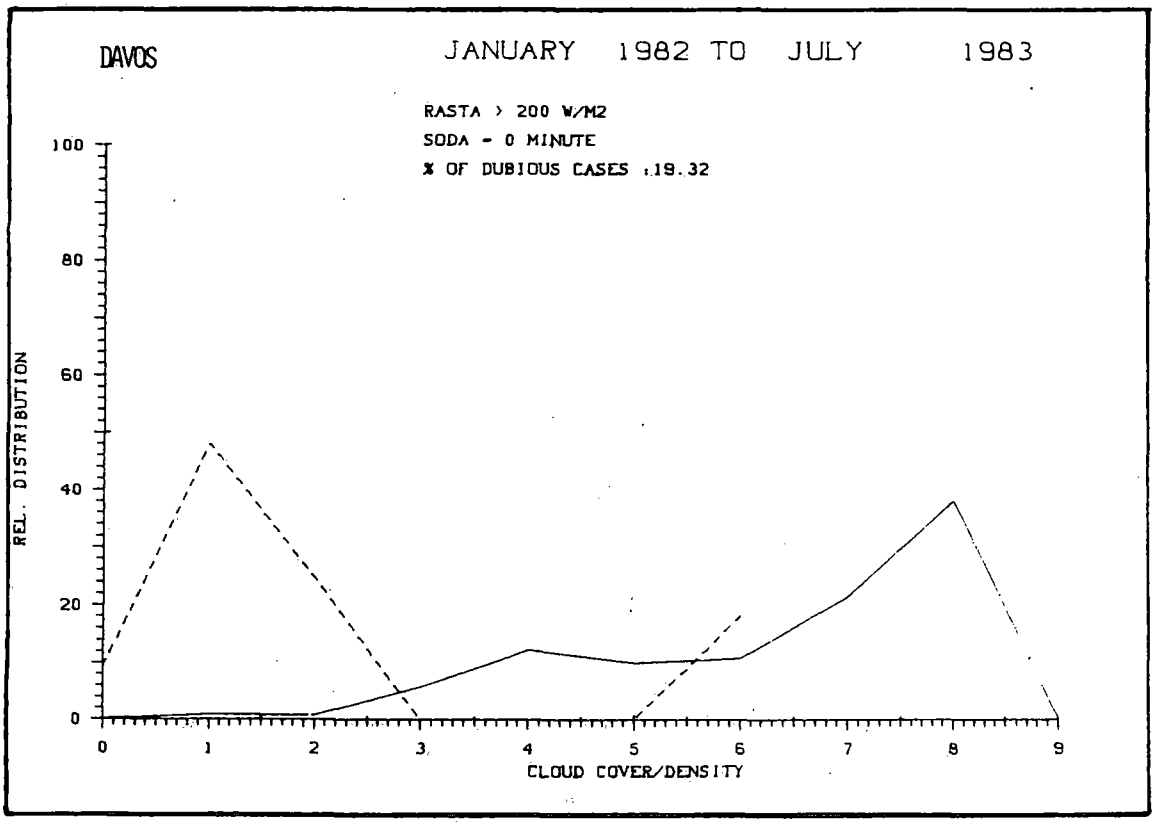

Fig. 2.6 Relative distribution of the sunshine duration dubious cases as function of the cloud cover (full line) and of the cloud opacity (broken line).
Cloud cover range: 0..8 (9: transmission errors).
Opacity scale : 0..5 (6: non-transmitted observations).

The fact that the problem seems to disappear in August 1983 can be explained by the replacement of the instrument at that time. It is clear that faulty instruments may not always be immediately detected. But the above investigation shows how important and instructive redundant measurements may be within an automatic network. The same software programs will be used for the next few years, but this time in order to check whether or not the replacement of the instrument did solve the problem.

3. GLOBAL RADIATION

Two pyranometers were available for the test period, and measurements are still being performed with this set-up. As mentioned in the introduction, the first unit is a routine instrument of the network. The second unit is a PSP Eppley Precision pyranometer belonging to the WRCD. The main difference between the two stems from the fact that only the first one is ventilated. This characteristic is important mainly in cases of frost or snowfalls since the second instrument has to be cleaned manually every morning by the WRCD staff. Otherwise, PSP and CM6 pyranometers belong to the same type of instruments. The Eppley Precision pyranometer, however, is temperature compensated and has very good cosine response (2). As the two instruments are mounted close to each other, they should record the same irradiance values. It is therefore justified to investigate the ratio of the intensities for each 10 minute interval. The result of this comparison is shown in figure 3.1, where different intensity classes are defined. The relative distribution of the ratios is rather broad for low intensities and gets narrower for ascending irradiance values. It is an interesting fact that the shape of the distribution changes for irradiances of about 600 W/m^2. The global irradiances are smaller for the ANETZ instrument under that level and higher above it. This suggests a scaling factor difference. However, all data above 200 W/m^2 lie in a range of ± 10% error. Values under this level must be treated with care because of the discrete character (low resolution) of the recorded values.

If we assume that the RASTA system is working properly, there is another way of controlling the quality of the pyranometer readings by computing the global irradiance with the help of the direct and the diffuse components. The ratio of the computed to the measured values as function of the computed intensity is shown on figure 3.2 for both instruments. The Eppley Precision pyranometer shows a better behaviour below 600 W/m^2 than the ANETZ instrument and this trend is reversed above that value, which confirms the preceding result. A closer look at the two curves suggests that the WRCD instrument might have some calibration factor problems (constant ratio deviation), but ortherwise works properly, while the ANETZ pyranometer seems to present a non-linear behaviour, a fact which has been often reported for the Kipp & Zonen instruments.

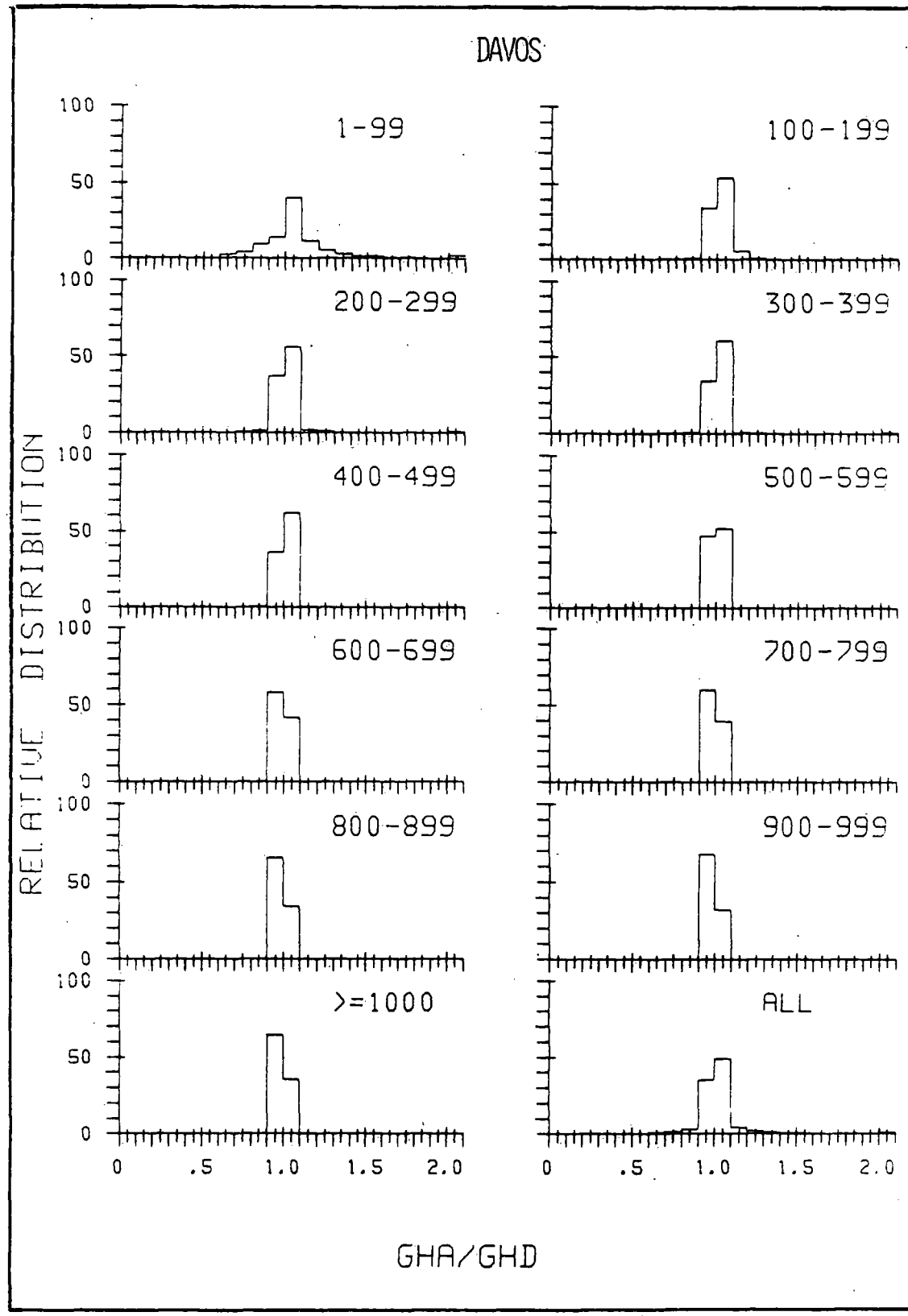

Fig. 3.1 Relative distribution of the ratio of the global irradiances measured by the two pyranometers for each 100 W/m^2 class recorded by the routine instrument. The last diagram (lower right) displays the distribution for the whole set of measurements.
Period: January 1982 to December 1983.

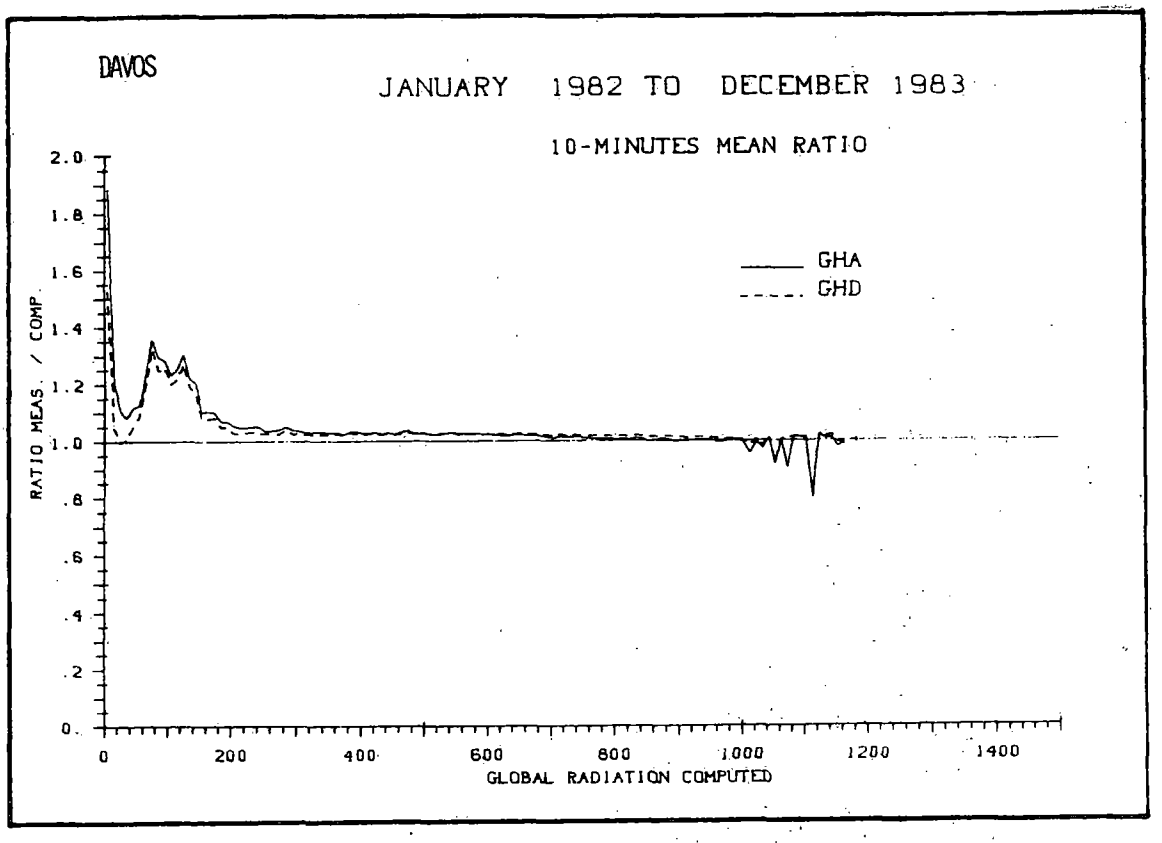

Fig: 3.2 Ratio of the measured to the computed global irradiances as function of the computed intensity.
Full line: routine pyranometer (Kipp & Zonen).
Broken line: reference pyranometer (Eppley PSP).

Problems arise for low irradiance values. The data above 1000 W/m^2 are not significant since they are due to rare events.

We may however conclude that both instruments work in a satisfying way for intensities lying between 200 and 1000 W/m^2. The light mismatching in the calibration factors and/or the non-linearity of the sensitivities leads to systematic deviations of opposite signs below and above about 600 W/m2. Going back to the simple ratios between instruments, figure 3.3 shows the behaviour of the mean value of the ratio for each available 10 W/m^2 interval (solid line) and the root mean square deviations of the mean. This result is equivalent to the preceding one: furthermore it illustrates the fact that the CM6 pyranometer is not linear and records higher values than its companion under 200 W/m^2 with an increasing magnitude as the intensity decreases. The increasing r.m.s deviation can be explained by the use of discrete values with a resolution of about 10 W/m^2/bit. The preceding fact can be further investigated by studying the diurnal behav-

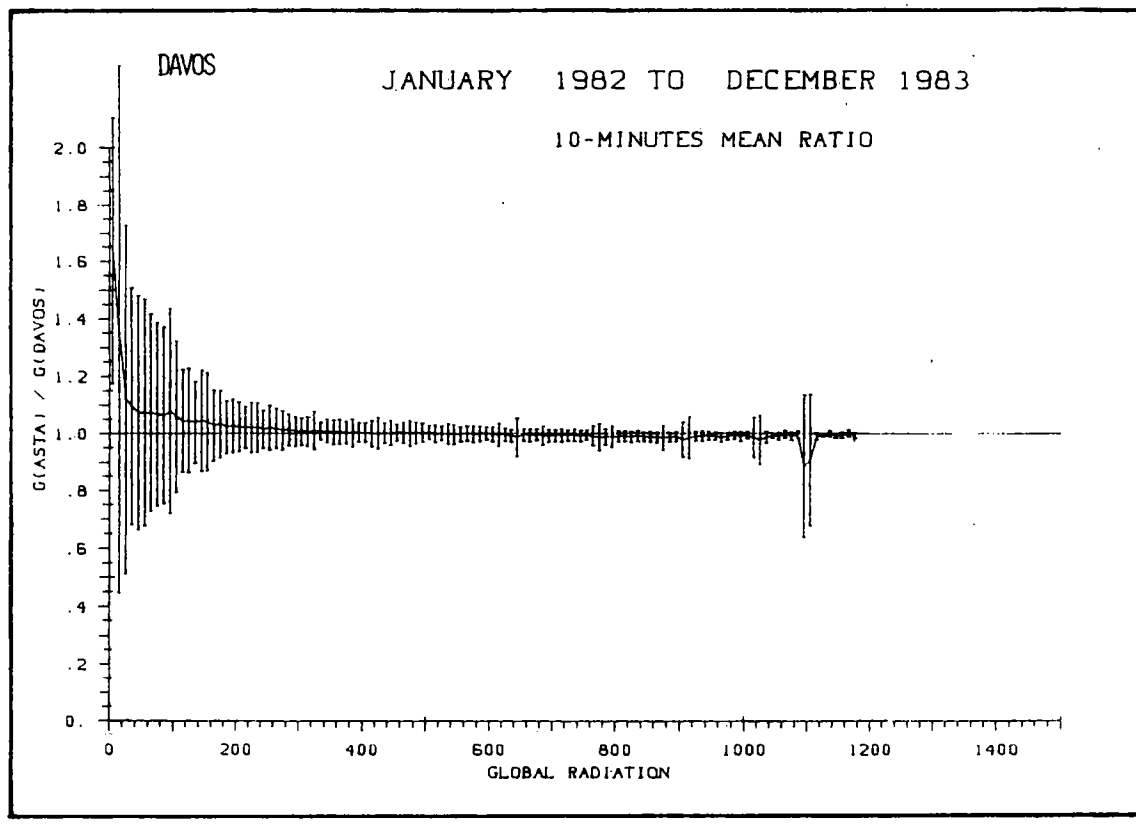

Fig. 3.3 Ratio of the irradiances measured by the global pyranometer (G(ASTA)) and the reference instrument (G(DAVOS)) as function of the reference global irradiance. The vertical bars indicate the standard deviation of the mean ratio (full line) per 10 W/m^2 intensity class.

aviour of the monthly mean ratio and its root mean square deviation, as shown on figure 3.4 for summer conditions: the mean ratio (solid line) shows values near unity but for the early and late hours where

- the irradiance intensities are low,
- the elevations of the sun are small.

This again confirms the preceding results.

Figure 3.5 shows the same kind of representation for winter conditions. The interesting fact is that up to 10 a.m., the deviation between the instruments is approximately + 10% with a strong r.m.s error, but decreases during the afternoon and increases again in the evening. This is most probably due to the occasional presence of snow, frost or ice on the non-ventilated instrument together with the low solar elevations and intensities.

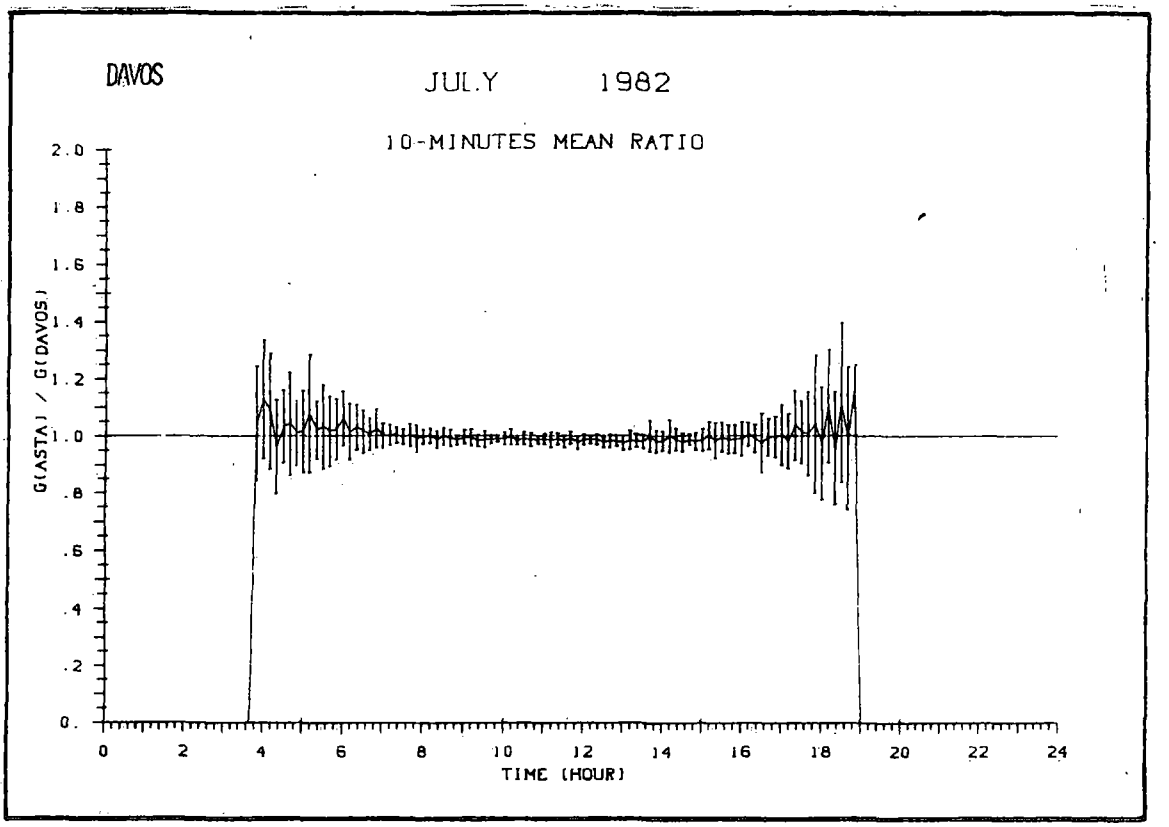

Fig. 3.4 Same as Fig. 3.3 as function of the time of the day for each 10 minute interval for a summer month.

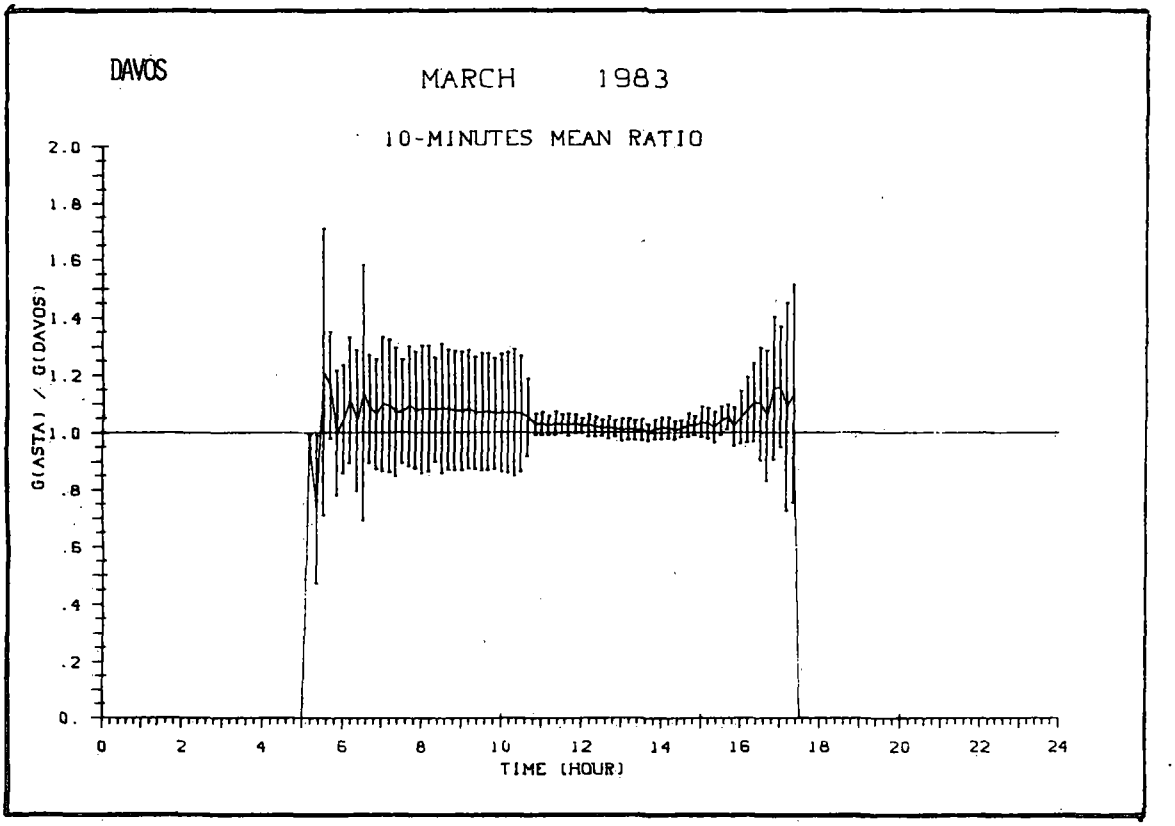

Fig. 3.5 Same Fig. 3.3 as function of the time of the day for each 10 minute interval for a winter month.

The following conclusions may now be drawn:

1. The CM6 pyranometer of the ANETZ network and the PSP Eppley pyranometer from the WRCD show results which are well correlated within the intensity range 200 ... 1000 W/m^2.

2. The intensity ratios of the two instruments display evident deviations for low intensities and low solar elevations where the ANETZ instrument tends to record higher values than the PSP due to non-linearities of the former.

3. In winter, care must be taken because one of the instruments is ventilated, avoiding therefore the disturbing presence of snow or ice on the glass hemispheres.

4. Comparisons with computed values obtained with other instruments show a slightly better behaviour of the WRCD pyranometer.

Taking into account the preceding conclusions, the PSP Eppley Precision instrument is chosen as reference for the following comparisons, though it is not ventilated and may therefore yield incorrect information in some cases, mostly in winter.

4. DIRECT RADIATION

The RASTA measuring system includes two main components: the automatic sun-tracker and the active cavity absolute radiometer PMO-6. The present section deals separately with the two units. The sun-tracker is a purely mechanical/electronical device and has to be controlled as such. The performance of the absolute radiometer depends on the pointing qualities of the sun-tracker and on the accuracy of the sensor.

4.1 The sun-tracker

The movements of the sun-tracker are controlled by a micro-processor which computes the position of the sun as function of the latitude of the site and declination of the sun on that particular day and time of the day. A position recorder is temporarily added for control purposes in order to check whether or not the computed angles are reached. Thus, the hour angle and declination deviations are stored every 10 minutes. Any clamping of the mechanism due to freezing temperatures, humidity or whatever reasons can be detected in this way. The relative frequency distribution of these deviations for a winter month is presented on figure 4.1. Considering the whole test period, the results are very satisfying and the sun-tracker can be regarded as operational from that point of view.

The fact that the tracking system is properly operating internally is necessary but not sufficient, the tracking accuracy has also to be tested. For that purpose, a four-quadrant sensor is added to the system and records the deviations from a perfect pointing. Detailed description of the computation may be found in (1). Figures 4.2 and 4.3 illustrate the shifting of the image of the sun through the four quandrants for a summer and a winter month respectively. Only periods with some sunshine are of course selected. The number of the day is written on the left upper corner of each graphic.

The general behaviour may be considered as excellent. The hour angle and declination deviations remain in a range of approximately $\pm$ 0.5 mm . This has to be related to the misalignment allowed from the optical construction of the radiometer. As the slope between the view limiting aperture and the entrance aperture amounts to 1.005 degres, the maximum possible deviation reaches approximately $\pm$ 0.75 degres. This shows that a proper set-up of the instrument

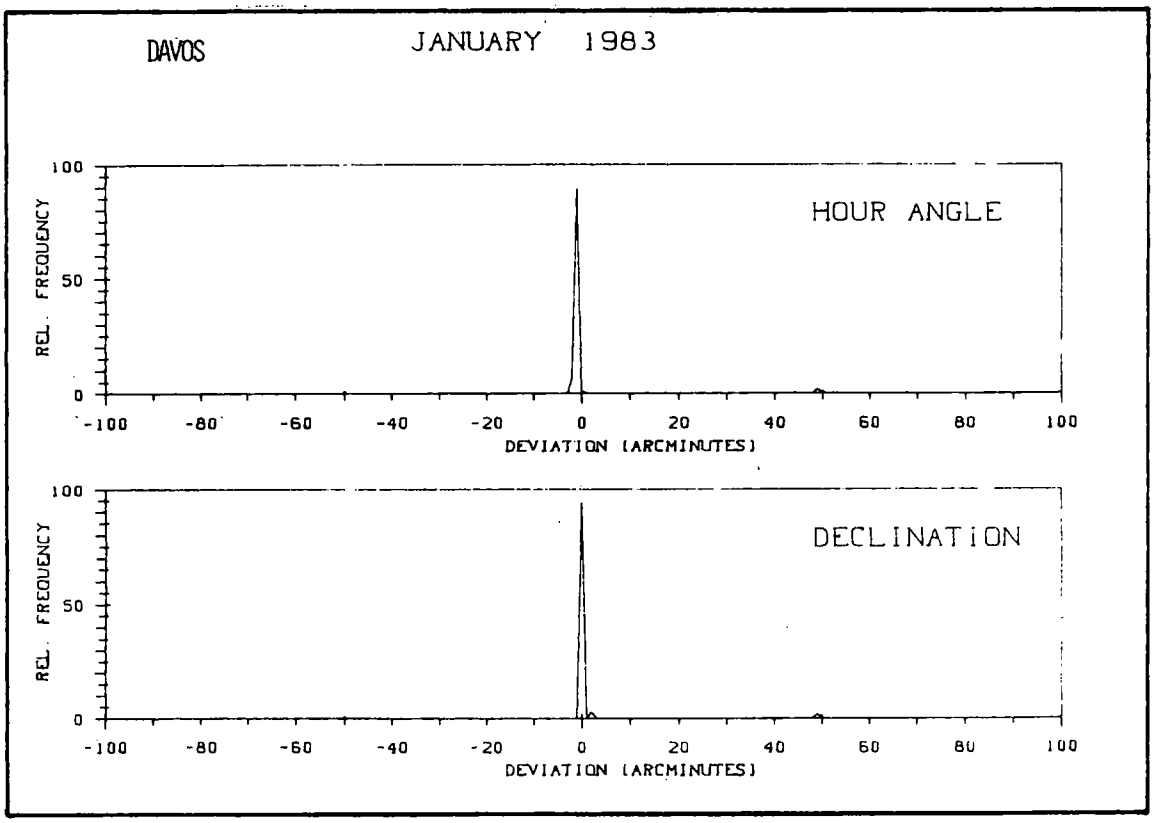

Fig. 4.1 Relative frequency distribution of the hour angle's (upper part) and declination's (lower part) deviations from the computed positions of the RASTA sun-tracker for a winter month.

and a very precise orientation are of utmost importance. The consequence of misalignment is a systematic trend in the motion of the image of the sun on the four quadrant sensor. Spherical geometry computations presented in (1) are used to determine the position errors of the sun-tracker due to misalignment towards south and the polar axis. The results are shown on figures 4.4 and 4.5 for the same months as before. In July 1982, the tilt angle seems to remain almost perfect while the azimuth deviation oscillates between -0.4 and -0.2 degrees. This has to be related to some electronic problems which were eliminated in September 1982. In January 1983, the situation looks more positive since both angles are of the order of -0.2 degrees.

Furthermore, the study of the whole test period shows that the deviations of both angles remain within the allowed alignment tolerance. Therefore, the complete mechanical construction of the sun-tracker may be considered as operational, as long as it remains properly oriented.

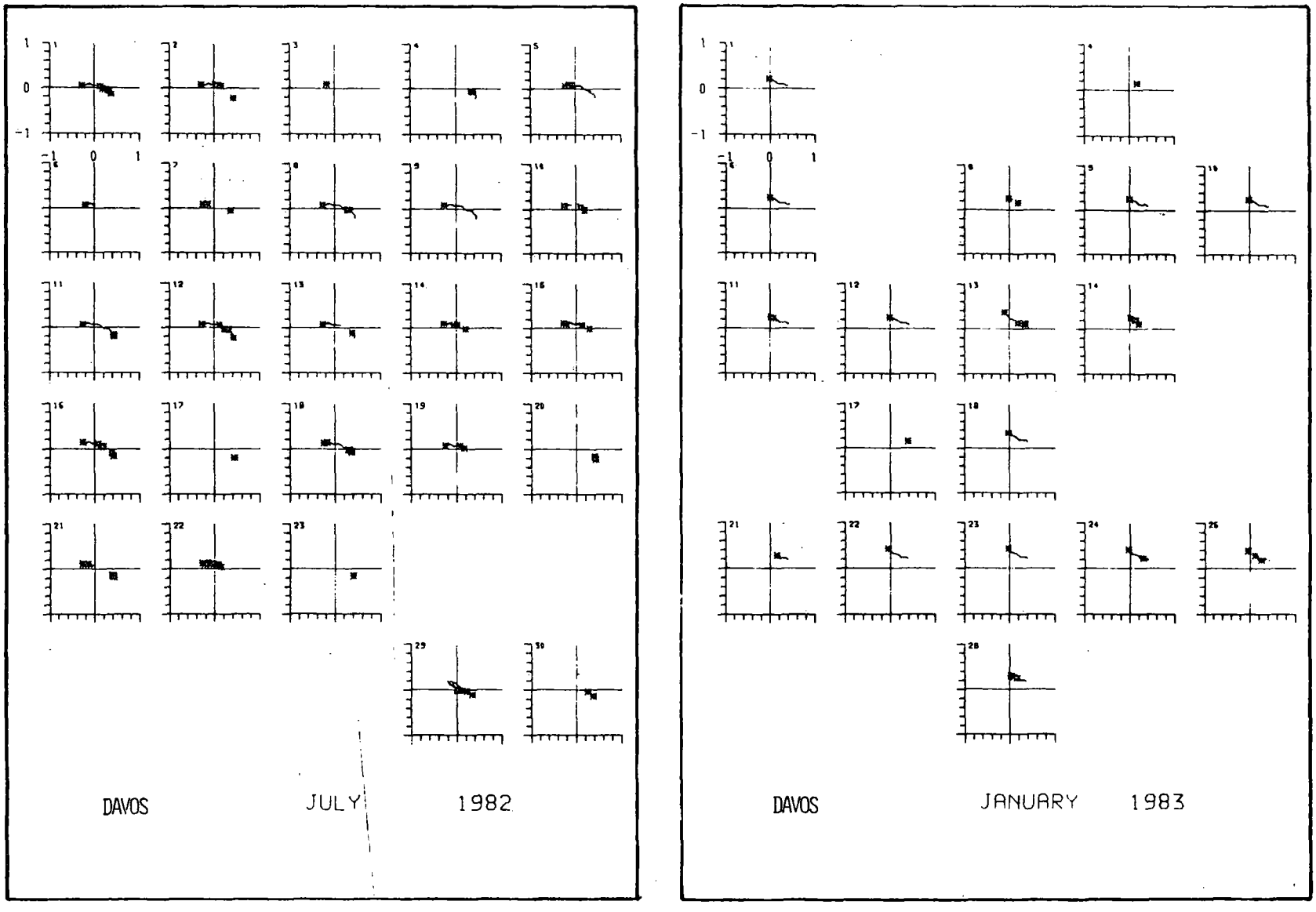

Fig. 4.2 and 4.3 Displacement of the image of the sun on the four-quadrant sensor fo the RASTA system for two different months. A star indicates the beginning of each uninterupted sunshine period. The daynumber is written on the left upper part of each diagram. The scale in [mm] is indicated on the first plot.

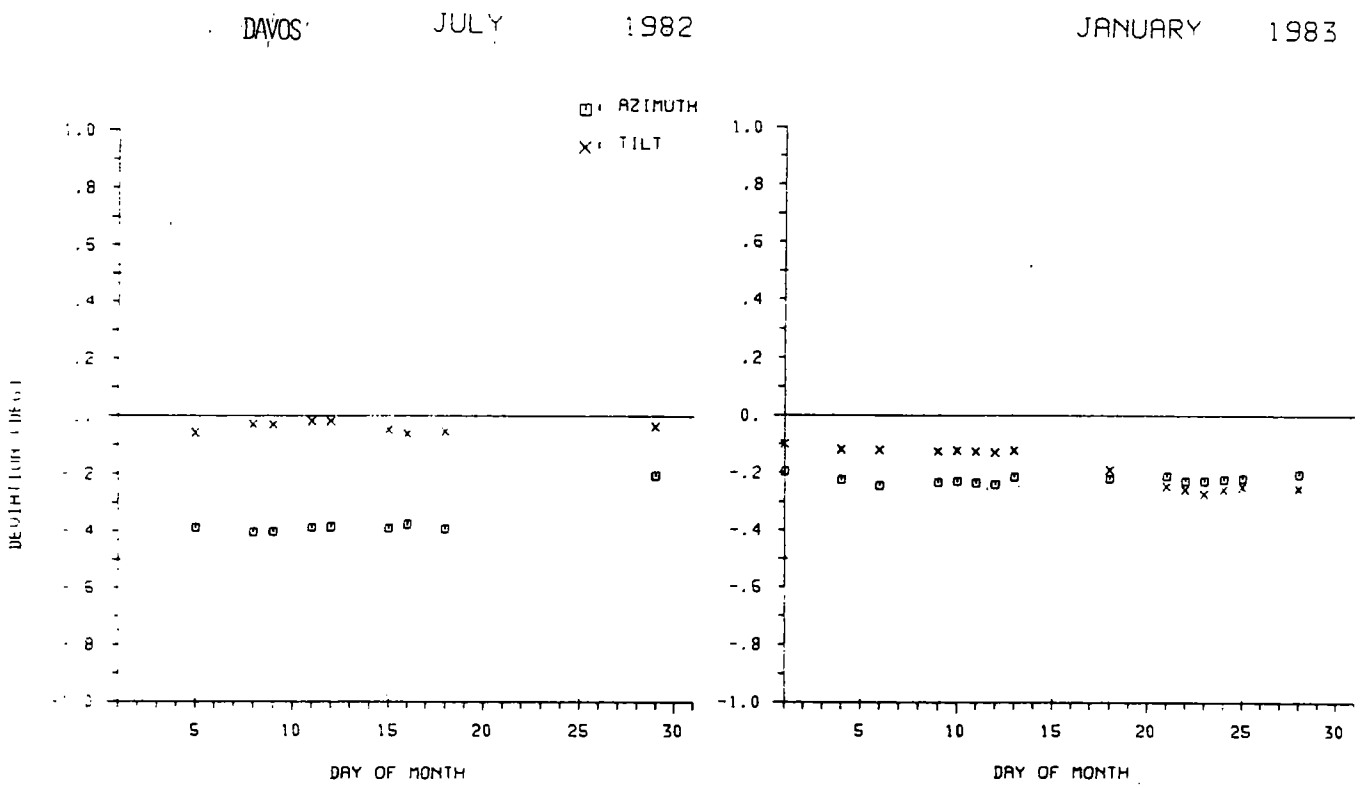

Fig. 4.4 and 4.5 Monthly variation of the deviation from an ideal positioning of the azimuth (geographical south) and tilt (latitude) angles of the RASTA sun-tracker for two different months. The values are computed from the four-quadrant sensor data (see Fig. 4.2 and 4.3).

4.2 The absolute radiometer

The absolute radiometer values for each 10 minute interval is the result of the integration of the irradiances measured for 20 groups. Each group consists of 6 readings representing the mean value of 100 analog/digital conversions, meaning that a total of 120 measurements are integrated at the end of the 10 minute period. For each separate group, the total system deviation is compared with a predetermined threshold and the group is rejected if it lies outside the tolerated boundaries. This information is coded in order to be contained in only one character (number of rejected groups + 2 divided by 3): 0 means that all the groups were accepted, 7 that they were all rejected, 8 that some hardware error occured and 9 that the sun-tracker was out of order.

DAVOS

RASTA REJECTED GROUPS STATISTIC

DATE		0	1	2	3	4	5	6	7	8	9	OUT	TRAN
JANUARY	1982	763	8	2	2	3	1	9	21	0	607	0	529
FEBRUARY	1982	1425	2	0	0	0	0	0	0	0	21	0	572
MARCH	1982	2115	18	1	0	0	0	0	0	0	29	0	83
APRIL	1982	2301	28	0	0	0	0	0	0	0	42	0	85
MAI	1982	2694	6	0	0	0	0	0	0	0	31	0	87
JUNE	1982	2744	0	0	0	0	0	0	0	0	0	0	100
JULY	1982	2764	6	2	4	3	5	3	8	3	0	0	94
AUGUST	1982	2573	0	0	0	0	0	0	0	0	0	0	79
SEPTEMBER	1982	1596	0	0	0	0	0	0	0	0	152	0	961
OCTOBER	1982	1693	1	0	0	0	1	4	1	0	214	0	204
NOVEMBER	1982	1261	0	0	0	0	0	0	0	0	78	0	932
DECEMBER	1982	1467	0	0	0	0	0	0	0	0	49	0	105
JANUARY	1983	1600	0	0	0	0	0	0	0	0	36	0	45
FEBRUARY	1983	1637	0	0	0	0	0	0	0	0	0	0	44
MARCH	1983	2156	0	0	0	0	2	0	0	0	0	0	57
APRIL	1983	2398	0	0	0	0	1	0	0	0	5	0	53
MAI	1983	2549	0	0	0	0	0	0	0	0	161	0	81
JUNE	1983	2741	0	1	0	0	35	0	0	0	2	0	61
JULY	1983	2555	2	0	1	0	76	0	0	7	180	0	46
AUGUST	1983	2556	3	0	1	0	22	0	0	1	6	0	49
SEPTEMBER	1983	2184	0	0	0	0	5	0	0	0	0	0	81
OCTOBER	1983	1943	0	1	0	0	35	0	0	0	0	0	45
NOVEMBER	1983	1575	0	0	0	0	0	0	0	9	52	0	71
DECEMBER	1983	1128	0	0	0	0	0	2	3	0	435	0	33

Table 4.1 Monthly statistic of the number of rejected measurement groups of the RASTA radiometer. The range extends from 0 to 9 (see explanations in text). Only diurnal cases are displayed.
Column "OUT" indicates that no value out of range was found during the whole test period.
Column "TRAN" displays the number of unavailable information mostly due to transmission errors.

Table 4.1 presents the montly occurrences of the rejected groups. Some problems appeared in January 1982 as well as from September to November 1982. Fig. 4.6 illustrates for September 1982 the temporal distribution of the faulty groups per day. Large errors occured on the 12th, between the 21st and the 22nd and on the 28th of that month. This information is constantly available and the dubious cases are automatically rejected for further evaluations.

We are now confident that the general behaviour of the sun-tracking system and of the internal fine adjustment of the radiometer are working in a satisfactory way. We also know that the reference pyranometer is yielding good quality results. Since the diffuse irradiance intensities are also recorded during the test period, a good

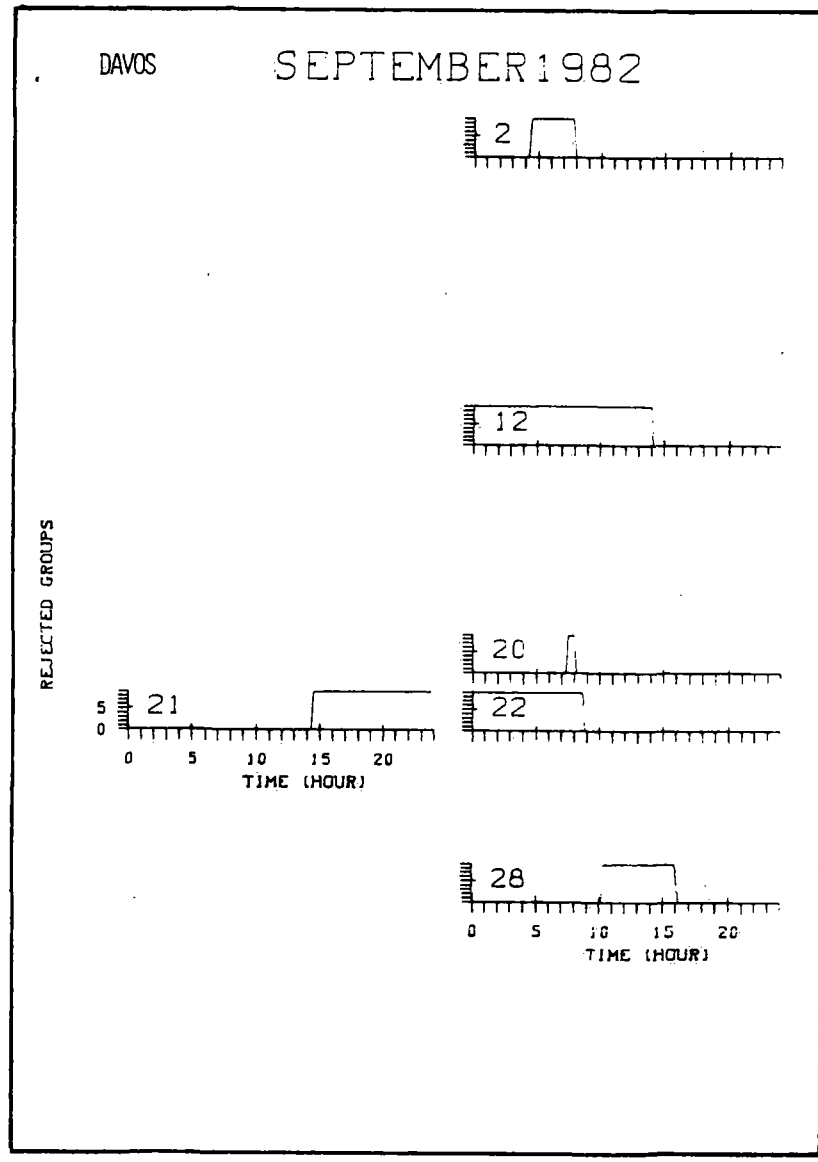

Fig. 4.6 Monthly distribution of the rejected group cases. Only days where rejections occured are displayed.

redundancy is available: by measuring the three parameters simultaneously, it is possible to check the instrument by:

1. computing the direct irradiance from the global and diffuse irradiances and comparing the results with the measured RASTA values,
2. computing the global irradiance from the direct and diffuse components and comparing the results with the measured global values,
3. computing the diffuse irradiance from the direct and global irradiances and comparing the results with the measured diffuse values.

The method is straightforward, but leads unavoidably to some problems since all three instruments are subject to uncertainties which in addition can be magnified by the multiplication through trigonometric functions of the sun's elevations. In fact, the problem lies in the way the errors on a specific instrument are going to propagate and influence the comparisons.

We have already seen in chapter 2 that the two pyranometers recording the global radiation are well correlated apart from the cases of low intensities. Thus it may be assumed that the global irradiance values are more or less accurate above a threshold value of approximately 200 W/m^2. Furthermore, the use of this reference is particularly valuable since all the ANETZ stations are equiped with such instruments. It is therefore interesting to see if some kind of systematic behaviour exists between the direct and the global irradiance values which could yield some algorithm suitable for the rejection of the cases where at least one of the instruments did not work properly.

Figure 4.7 shows the mean direct irradiance values per global irradiance class of 50 W/m^2. The vertical bars represent the root mean square deviation of the means. All the points are considered with the following restrictions:

- the sun elevation is higher than 0 degree,
- no transmission error occured,
- the number of rejected groups is smaller than 8,
- the computed or measured direct irradiances are higher than 2 W/m^2.

Figures 4.8, 4.9 and 4.10 show the same kind of representation with the further restriction that the sunshine duration is limited to 0, 1 to 9 and 10 minutes per 10 minute interval.

The "no-sun" case (figure 4.8) illustrates the problems linked to the poor behaviour of the sunshine recorder since no direct intensities above 200 W/m^2 should be present.

The rather smooth behaviour of the direct irradiance versus the global irradiance suggests the following quality tests:

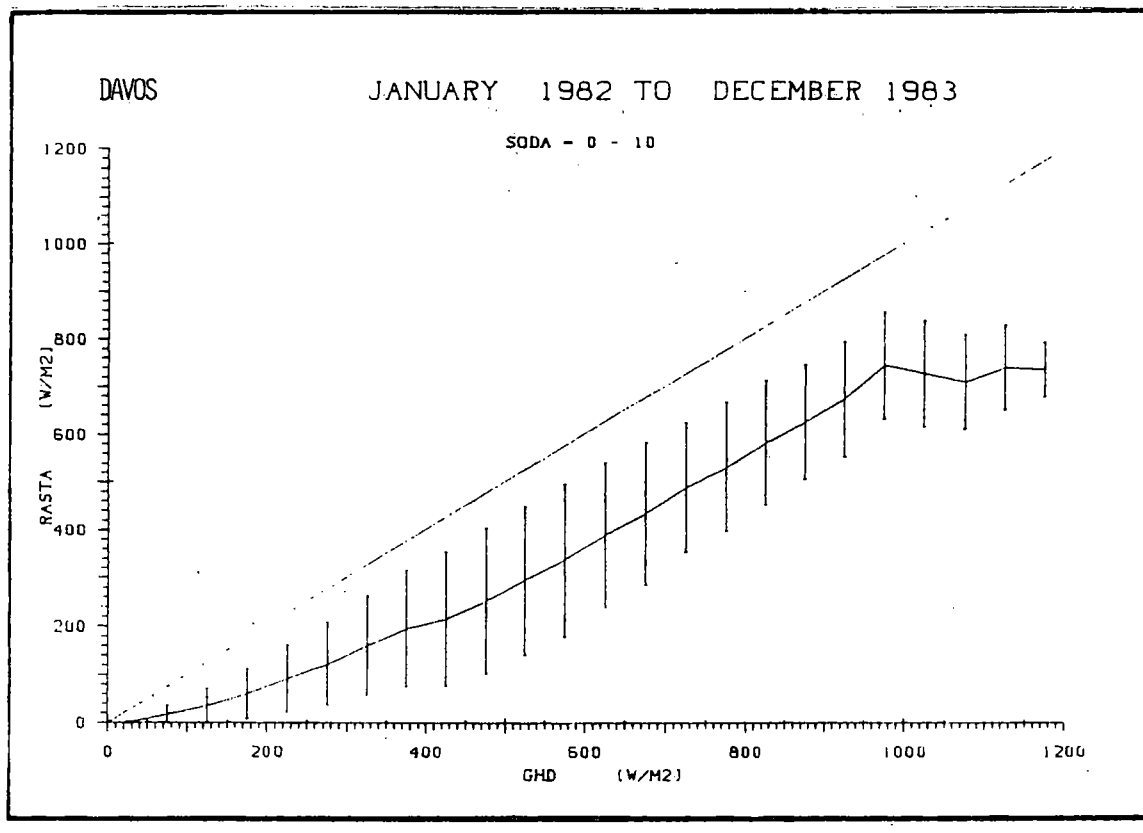

Fig. 4.7 Mean direct irradiance values as function of the measured global irradiance for the whole test period for all sunshine duration cases. Global irradiance classes of 50 W/m^2 are selected. The vertical bars indicate the standard deviation of the means.

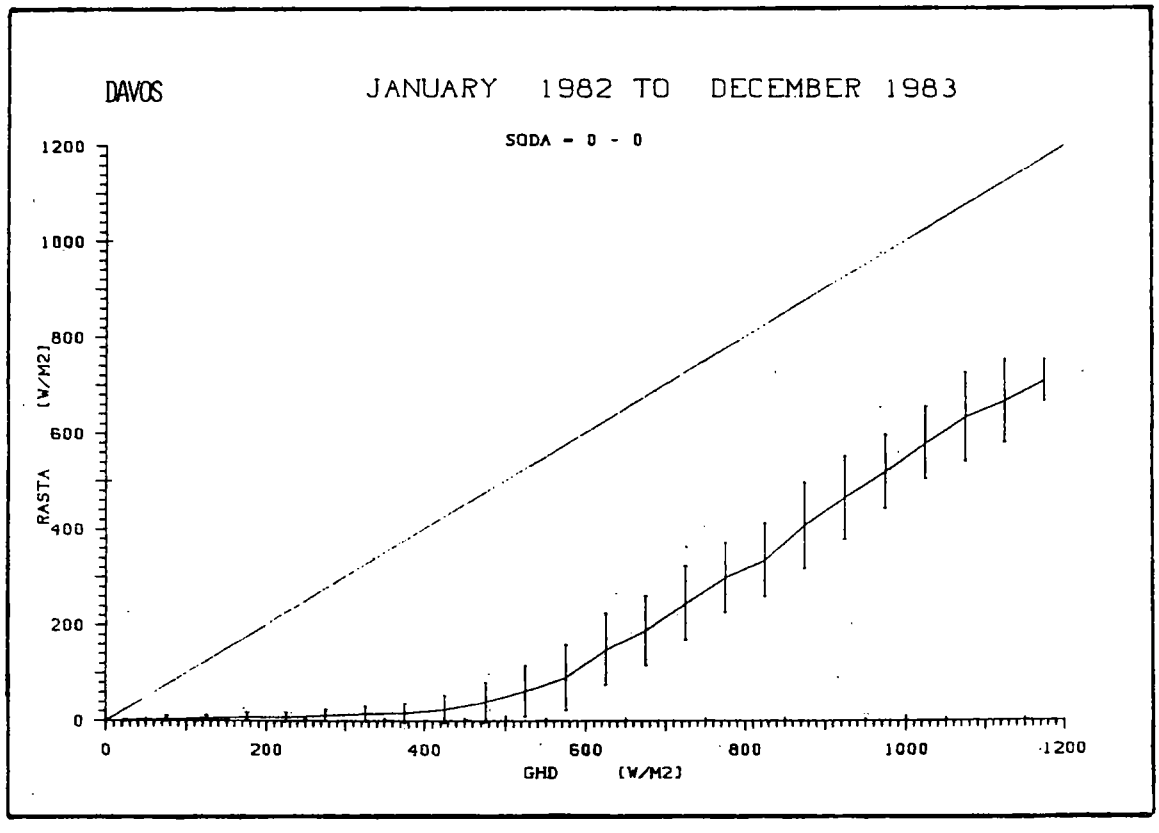

Fig. 4.8 Same as Fig. 4.7 for cases where no sunshine was recorded. The plot reflects the problems related to the poor behaviour of the sunshine instrument.

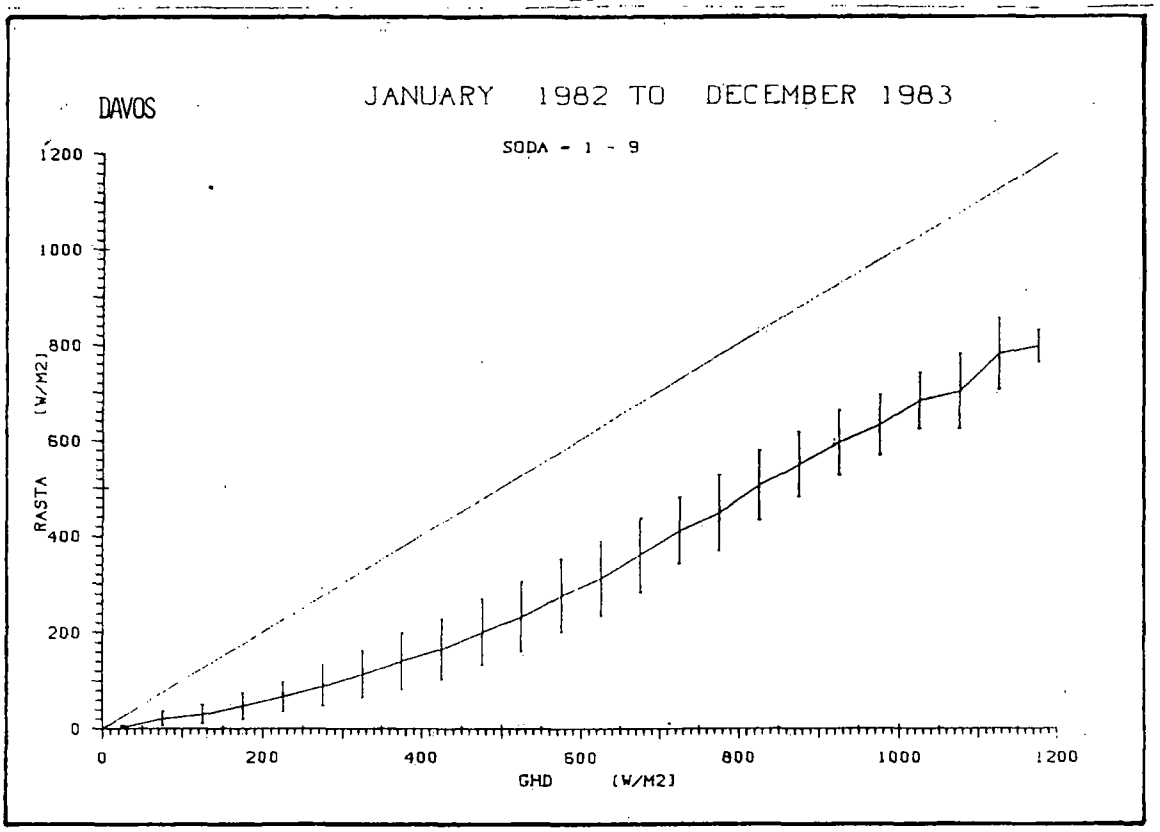

Fig. 4.9 Same as Fig. 4.7 for sunshine durations from 1 to 9 minutes.

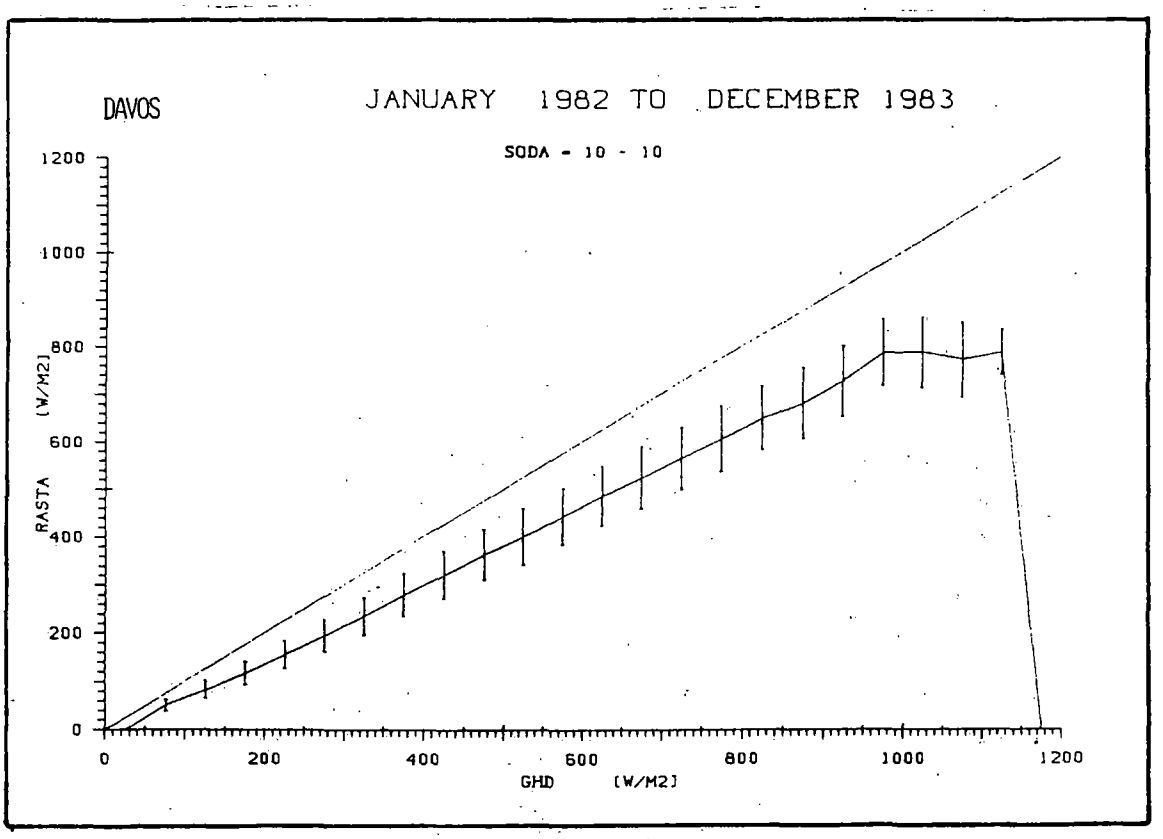

Fig. 4.10 Same as Fig. 4.7 for full sun cases only.

1. All the cases within the boundaries of the standard deviation are considered as fit for subsequent evaluations. A further criterion is applied to reject the cases where the difference between computed and measured direct intensities is higher than 100%. In this way all the cases where one of the instruments did not behave properly, but remained within the standard deviation limit (snow on the pyranometers, clamping of the RASTA, ...) are suppressed.

2. Values outside the standard deviation boundaries are rejected only if the difference between computed and measured irradiance is higher than 25%. This second level test takes into account special atmospheric conditions where the intensities are lying outside the standard deviation limits, but show a good agreement between themselves.

3. All the cases where the global irradiances from both pyranometers show a difference of more than 20% are rejected.

We are confronted with the following problem: since we know that the global irradiance values are more or less accurate, the deviations between the measured and computed direct irradiances have to originate either from the direct or the diffuse component. We know that

$$I = (Gh - Dh) \,/\, \sin(h)$$

therefore if Gh is considered free of errors, we have

$$\Delta I \cdot \sin(h) = \Delta Dh$$

or

$$\frac{\Delta I \cdot \sin(h)}{Dh} = \frac{\Delta Dh}{Dh}$$

and

$$\frac{\Delta Dh}{Dh} = \frac{\Delta I}{I} \frac{I \cdot \sin(h)}{Dh}$$

which means that a systematic error on the measured direct irradiance will propagate itself on the computed diffuse component by being modulated through the ratio of the direct to the diffuse components whose values can extend from 0 to more than 15 for extremely clear cases. In other words, a comparison between the measured and

the computed diffuse irradiances will indicate if either the RASTA or the diffuse pyranometer present some kind of systematic deviation.

Figures 4.11 to 4.14 show the results of such a comparison for the same sunshine duration classes as above. The conclusion is obvious: the diffuse pyranometer presents a tendency to measure values smaller than the computed ones and this behaviour remains more or less constant over most of the range of the direct irradiance. We may therefore assume that all the measured diffuse irradiances are to be corrected upwards and a mean value of +5% is chosen. This represents of course a minor correction, but it may be significant for low solar elevations. This underestimation tends to disappear for the clear situations (sunshine duration = 10 minutes) and high direct irradiances, i.e. high global intensities. In this case, a small deviation of the diffuse component will be insignificant compared with the possible uncertainties of the direct and the global measurements since the modulation factor mentioned above will have the opposite effect.

We are now confident that the direct irradiance measurements show a very good behaviour and we may proceed to the last test by comparing the computed and measured direct irradiances, once the rejection tests 1. to 3. and the above correction of the diffuse irradiance are performed. The results are shown in figures 4.15 to 4.18 for the same sunshine duration categories as above and are positive, although there still seems to be some problems for low intensities. However, it must be kept in mind that both the global and the direct measurements may still present some uncertainties especially for low values where the digitalization effect plays an important role.

Other valuable information about the quality of the RASTA system can be gathered by the study of the rejection algorithm results. This is shown in table 4.2.

The first sub-table on the upper left part concerns all sunshine durations. Substracting all cases where the sun is below the horizon leaves 52891 points for the comparison. Successively, we compute that

- 3.8% of the left values have not been transmitted, leaving 50883 cases,

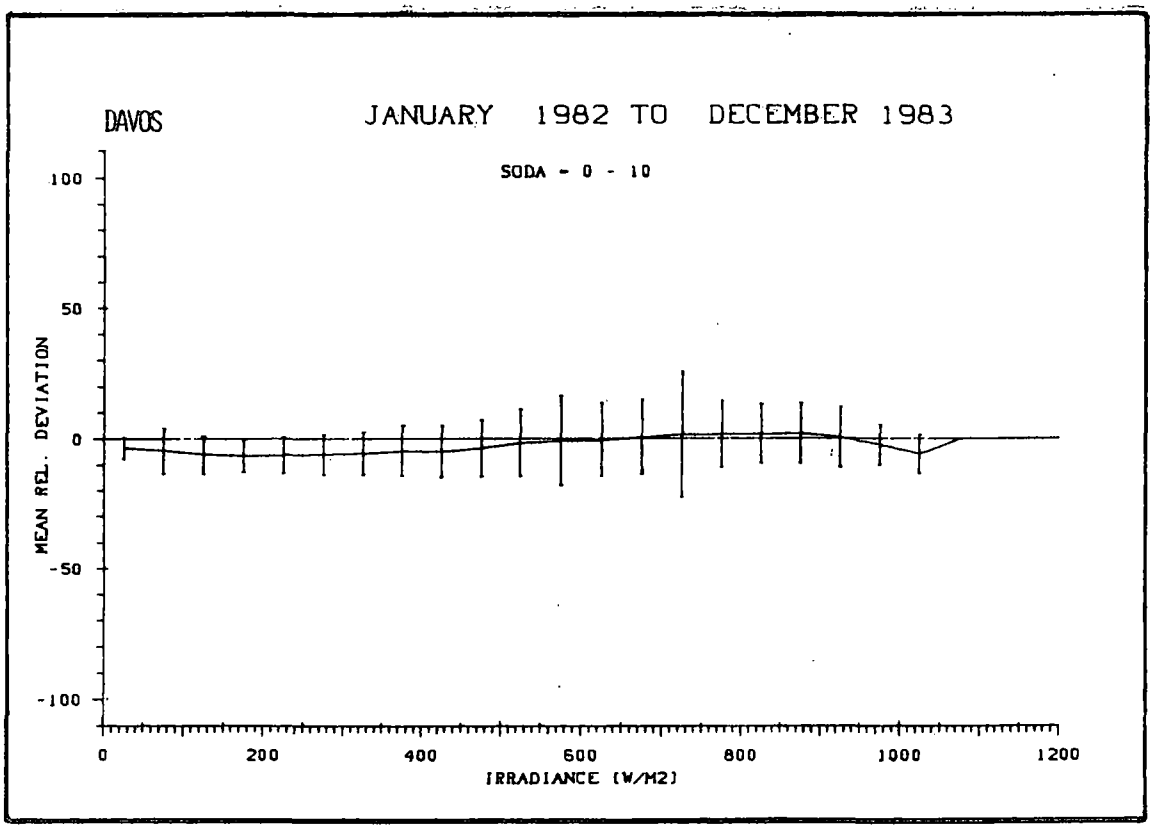

Fig. 4.11 Mean relative deviation of the measured diffuse irradiance from the computed diffuse irradiance as function of the direct irradiance for the same sunshine durations as in Fig. 4.7. The vertical bars indicate the standard deviation of the means.

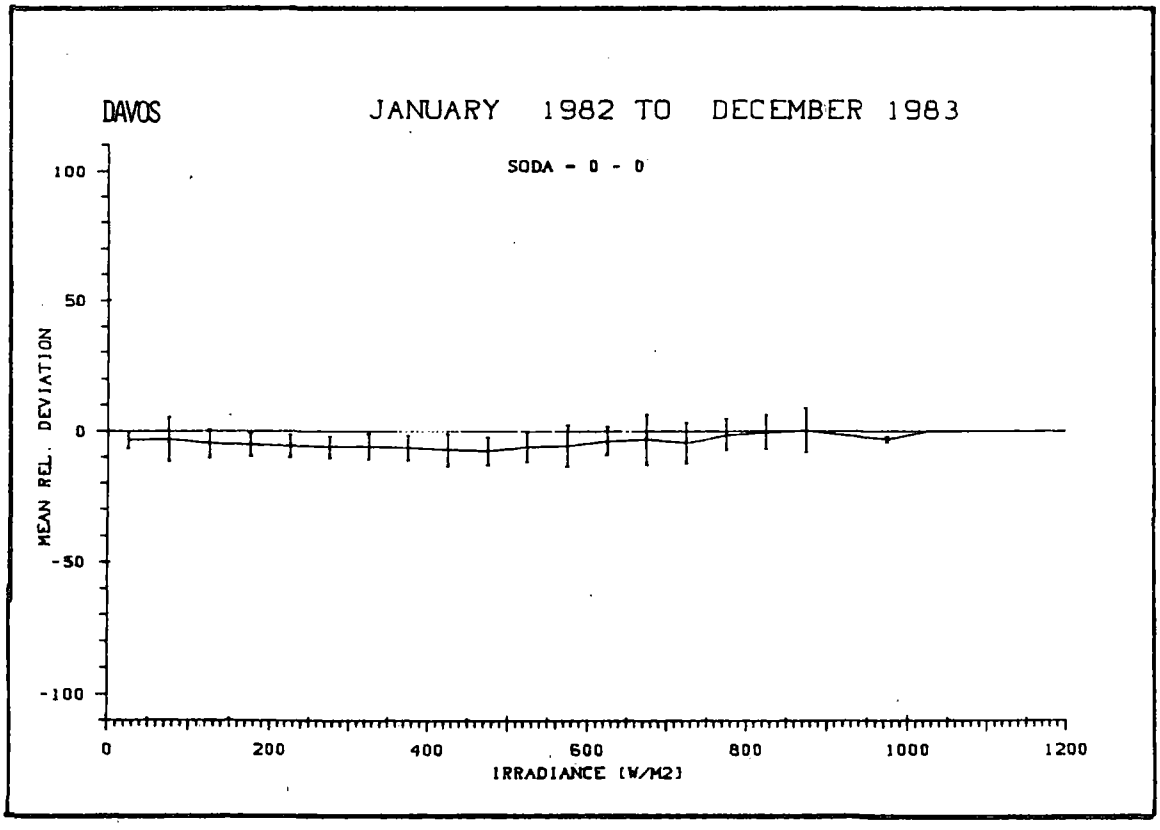

Fig. 4.12 Same as Fig. 4.11 for the same sunshine duration as in Fig. 4.8.

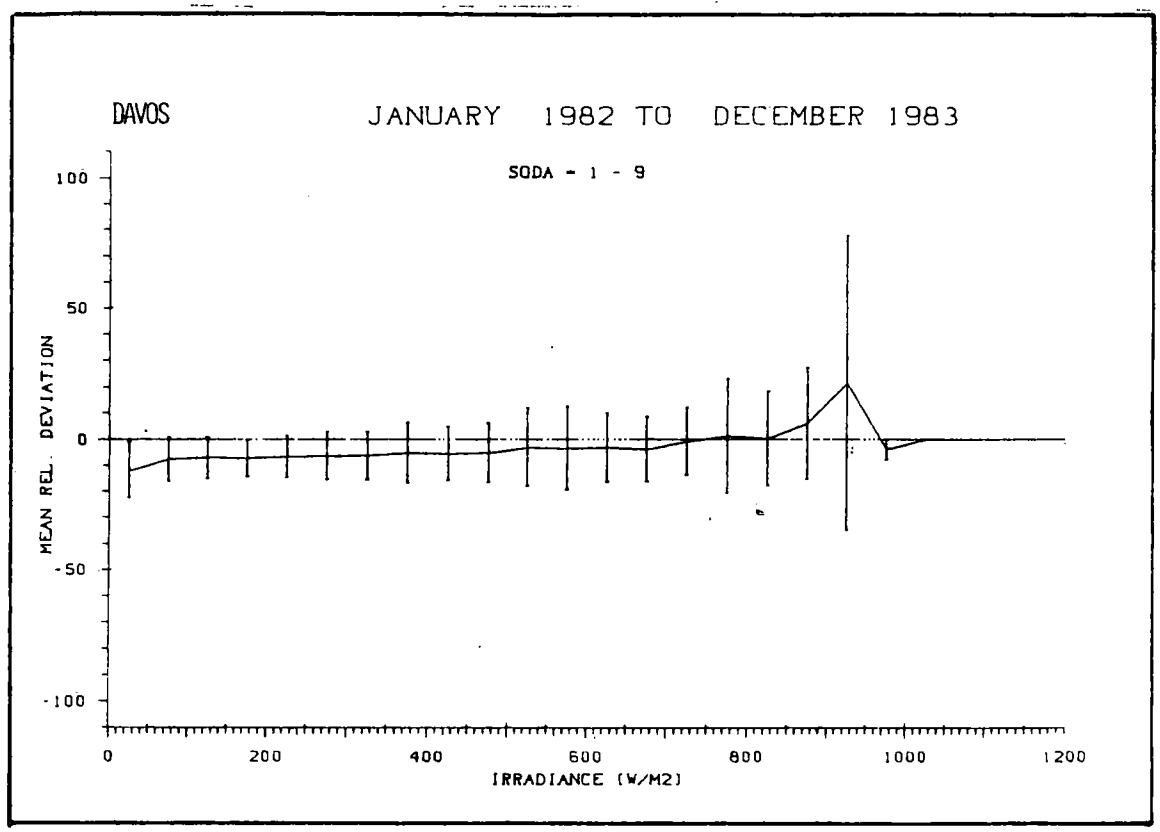

Fig. 4.13 Same as Fig. 4.11 for the same sunshine duration as in Fig. 4.9.

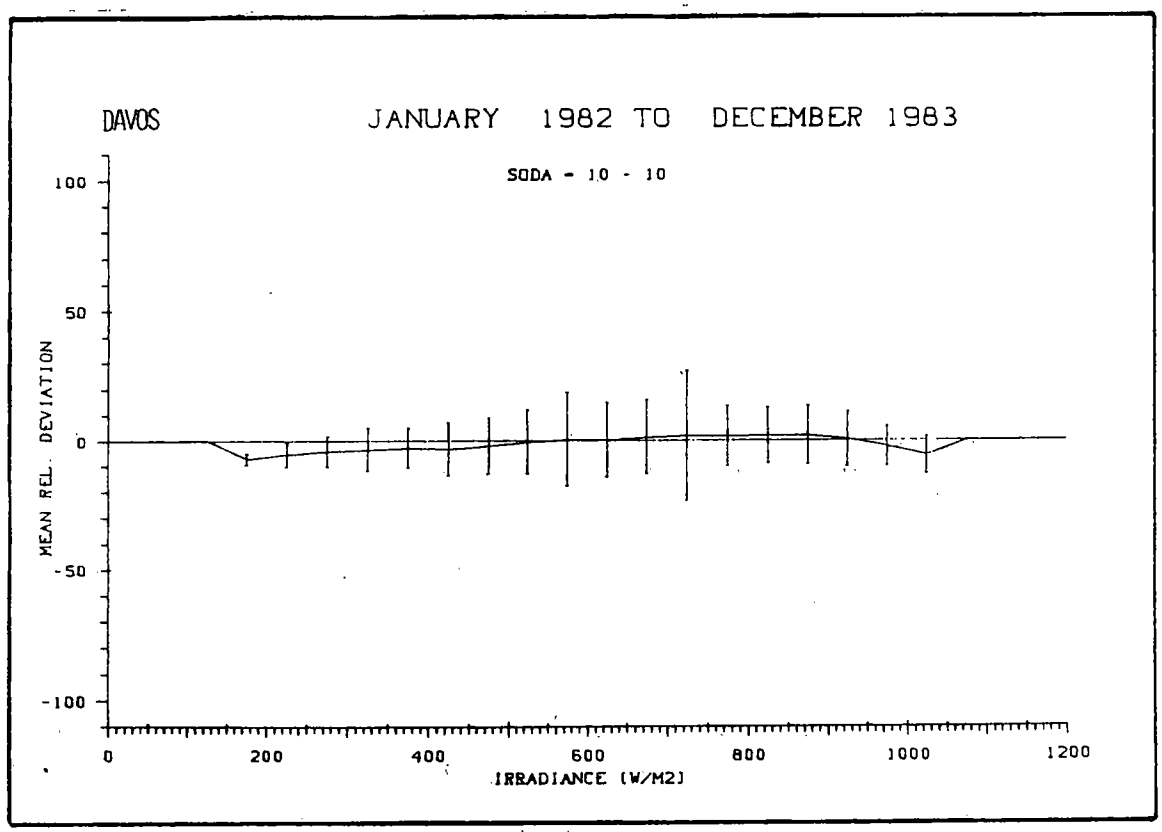

Fig. 4.14 Same as Fig. 4.11 for the same sunshine duration as in Fig. 4.10.

DAVOS — STATISTICAL RESULTS

SODA = 0 TO 10 MIN

TOTAL NUMBER OF POINTS	105408	
SUN <= 0.0	52517	
RASTA NOT TRANSMITTED	1847	
DASTA NOT TRANSMITTED	161	
RASTA OUT OF RANGE	2112	
ZERO INTENSITY	23800	
REJECTED SODA	63	
UNMATCHED GM	304	
I DEVIATION > 100%	1091	
NB. OF COMPARED CASES	22489	
REJECTED CASES	1024	4.6 %

RANGE	POINTS NB.	MEAN	ST. DEVIAT.	% REJECTED
25.0	1465	7.4	44.4	17.5
75.0	978	-1.9	32.8	19.9
125.0	793	-8.3	24.0	10.0
175.0	661	-7.9	18.7	7.1
225.0	646	-6.0	16.0	4.9
275.0	574	-4.5	13.8	4.7
325.0	592	-3.5	11.7	3.4
375.0	667	-1.9	10.6	2.7
425.0	703	-1.5	9.4	2.0
475.0	804	-.5	8.0	2.1
525.0	902	.6	7.0	.8
575.0	1077	.6	7.4	11.9
625.0	1250	1.1	5.3	.6
675.0	1442	1.3	4.3	.8
725.0	1617	1.2	3.8	.9
775.0	1871	1.4	3.1	6.5
825.0	2094	1.2	2.7	1.2
875.0	2113	1.0	2.0	.7
925.0	1605	.6	1.5	2.1
975.0	615	.2	1.1	.1
1025.0	20	-.3	1.1	.1
1075.0	0	0.0	0.0	0.0
1125.0	0	0.0	0.0	.1
1175.0	0	0.0	0.0	0.0

DAVOS — STATISTICAL RESULTS

SODA = 0 TO 0 MIN

TOTAL NUMBER OF POINTS	105408	
SUN <= 0.0	52517	
RASTA NOT TRANSMITTED	1847	
DASTA NOT TRANSMITTED	161	
RASTA OUT OF RANGE	2112	
ZERO INTENSITY	23800	
REJECTED SODA	20152	
UNMATCHED GM	90	
I DEVIATION > 100%	465	
NB. OF COMPARED CASES	3918	
REJECTED CASES	346	8.8 %

RANGE	POINTS NB.	MEAN	ST. DEVIAT.	% REJECTED
25.0	1367	8.7	45.0	25.4
75.0	678	2.8	30.7	26.3
125.0	388	-5.2	19.9	13.9
175.0	273	-6.3	17.0	6.8
225.0	221	-5.8	13.4	4.9
275.0	173	-5.3	10.7	2.3
325.0	162	-4.1	10.2	.9
375.0	125	-3.8	8.6	.9
425.0	115	-4.8	9.1	.6
475.0	87	-4.1	7.5	.3
525.0	72	-2.2	7.4	0.0
575.0	78	-1.2	6.5	2.6
625.0	56	.5	4.6	0.0
675.0	35	.8	7.0	.1
725.0	31	-.2	4.9	0.0
775.0	26	-2.0	3.6	11.0
825.0	19	2.5	3.8	0.0
875.0	7	3.0	5.0	0.0
925.0	2	1.5	.1	.3
975.0	3	.6	.4	0.0
1025.0	0	0.0	0.0	0.0
1075.0	0	0.0	0.0	0.0
1125.0	0	0.0	0.0	0.0
1175.0	0	0.0	0.0	0.0

DAVOS — STATISTICAL RESULTS

SODA = 1 TO 9 MIN

TOTAL NUMBER OF POINTS	105408	
SUN <= 0.0	52517	
RASTA NOT TRANSMITTED	1847	
DASTA NOT TRANSMITTED	161	
RASTA OUT OF RANGE	2112	
ZERO INTENSITY	23800	
REJECTED SODA	19624	
UNMATCHED GM	71	
I DEVIATION > 100%	418	
NB. OF COMPARED CASES	4397	
REJECTED CASES	461	10.5 %

RANGE	POINTS NB.	MEAN	ST. DEVIAT.	% REJECTED
25.0	98	-10.1	29.7	19.7
75.0	300	-12.7	34.8	24.1
125.0	405	-11.3	27.0	11.7
175.0	383	-9.9	19.9	7.8
225.0	401	-6.4	17.5	6.3
275.0	338	-4.9	15.7	7.2
325.0	320	-4.3	12.5	5.2
375.0	343	-2.6	12.2	3.9
425.0	290	-1.9	10.0	1.3
475.0	268	-1.7	8.9	1.1
525.0	252	-.6	8.2	.4
575.0	228	-.8	8.7	5.4
625.0	223	.3	7.1	.2
675.0	178	-.1	5.5	.4
725.0	150	1.3	5.2	0.0
775.0	118	1.3	5.2	5.0
825.0	67	.9	5.0	.2
875.0	23	2.4	4.6	0.0
925.0	7	2.7	3.5	0.0
975.0	5	.2	1.5	0.0
1025.0	0	0.0	0.0	0.0
1075.0	0	0.0	0.0	0.0
1125.0	0	0.0	0.0	0.0
1175.0	0	0.0	0.0	0.0

DAVOS — STATISTICAL RESULTS

SODA = 10 TO 10 MIN

TOTAL NUMBER OF POINTS	105408	
SUN <= 0.0	52517	
RASTA NOT TRANSMITTED	1847	
DASTA NOT TRANSMITTED	161	
RASTA OUT OF RANGE	2112	
ZERO INTENSITY	23800	
REJECTED SODA	10229	
UNMATCHED GM	143	
I DEVIATION > 100%	208	
NB. OF COMPARED CASES	14174	
REJECTED CASES	217	1.5 %

RANGE	POINTS NB.	MEAN	ST. DEVIAT.	% REJECTED
25.0	0	0.0	0.0	0.0
75.0	0	0.0	0.0	0.0
125.0	0	0.0	0.0	0.0
175.0	5	-8.7	6.9	1.4
225.0	24	-2.9	10.6	1.9
275.0	63	-.4	9.6	2.2
325.0	110	.0	10.6	3.7
375.0	199	.5	8.1	2.2
425.0	298	.1	8.6	5.5
475.0	449	.9	7.2	7.4
525.0	578	1.4	6.2	2.8
575.0	771	1.1	6.9	40.6
625.0	971	1.3	4.8	2.3
675.0	1229	1.5	4.0	2.3
725.0	1436	1.2	3.7	4.1
775.0	1727	1.4	2.9	2.8
825.0	2068	1.2	2.5	5.1
875.0	2083	1.0	1.9	3.2
925.0	1596	.6	1.5	9.2
975.0	607	.2	1.1	.5
1025.0	20	-.3	1.1	.5
1075.0	0	0.0	0.0	0.0
1125.0	0	0.0	0.0	.5
1175.0	0	0.0	0.0	0.0

Table 4.2 Statistical results of the comparison between computed and measured direct irradiances. The upper part of each sub-table gives an overview of the selection procedure. The lower part presents the distributions displayed on Figures 4.15 to 4.18.

- 4.2% of the left RASTA values have more than 7 rejected groups, leaving 48771 cases,
- 48.8% of the left cases have direct intensities less than 2 W/m^2, leaving 24971 cases,
- 0.3% of the left cases have a sunshine duration outside the possible boundaries (0 to 10 minutes), leaving 24908 cases,
- 1.2% of the remaining points have global irradiances which show more than 20% difference between the two instruments, leaving 24604 cases,
- 4.4% of the left cases show a deviation between computed and measured direct irradiances of more than 100%, which means that at least one instrument did not work properly, leaving 23513 cases.

Using the algorithm described above yields the rejection of 4.6% of the remaining cases where either the RASTA system itself or the comparison method did not work properly; 22489 cases remain for comparison. The rest of the table shows the distribution of the mean values of the deviation between computed and measured direct intensities, classified in 24 measured intensity steps of 50 W/m^2. The standard deviation is also included. The last column indicates the relative distribution of the 4.6% rejected cases. These results are displayed on figure 4.15 by the broken line which has to be referred to the left ordinate axis. More than half of the rejected values are contained in classes below 200 W/m^2. The peaks which appear for rather high intensities are due to the clamping of the instrument, since the last buffered value is repeatedly sent to the central station. This problem could be corrected in the future by setting the number of rejected groups to 9 for such cases.

The other three sub-tables of table 4.2 deal with the same statistics applied to specific sunshine duration values (figures 4.16 to 4.18). The best results are of course obtained for full-sun conditions where only 1.5% of the cases are rejected and where 40.6% of these 217 rejected cases are due to the blocking of the instrument.

The tendency to obtain negative mean deviation values together with high standard deviations for low intensities could be further decreased by adjusting the correction of the diffuse pyranometer. We

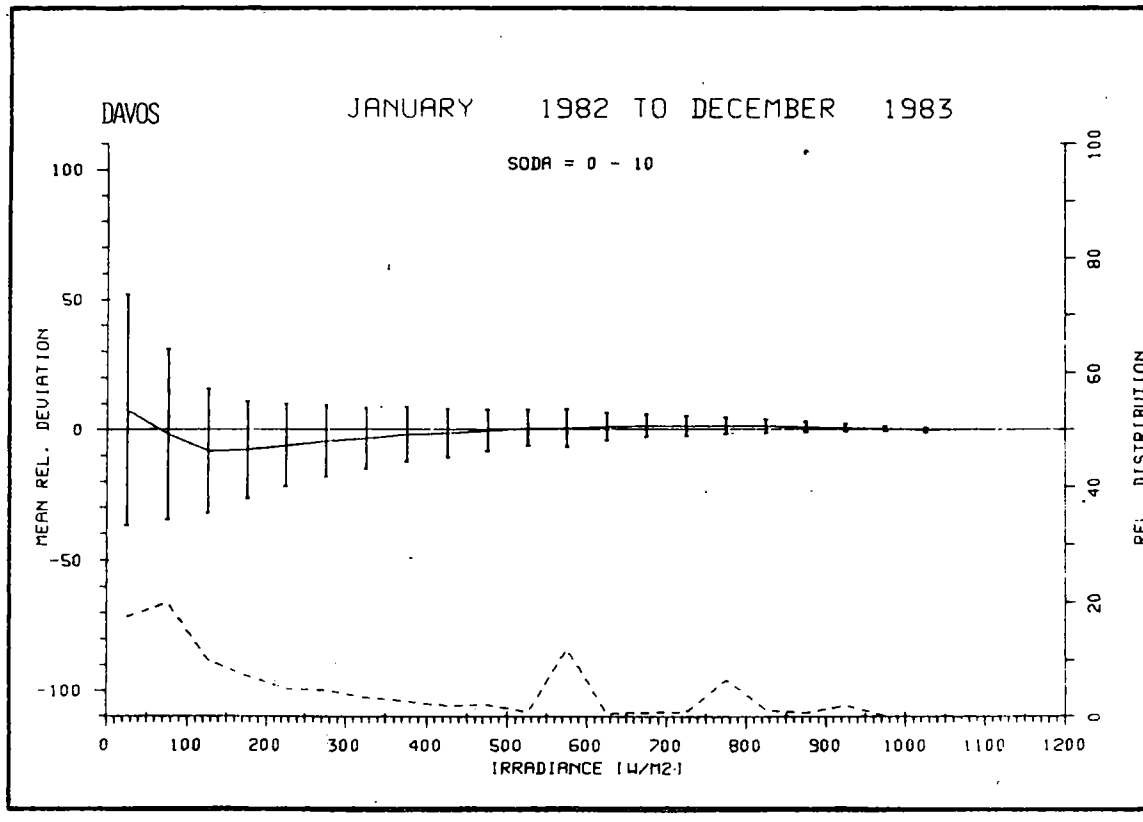

Fig. 4.15 Comparison between computed and measured direct irradiance as function of the measured direct irradiance for all sunshine durations. The measured diffuse irradiance used for the computation is corrected as explained in text. The vertical bars indicate the standard deviation of the mean. The dashed curve is related to the left ordinate and displays the relative distribution of the rejected cases presented in Table 4.2 (column "% REJECTED").

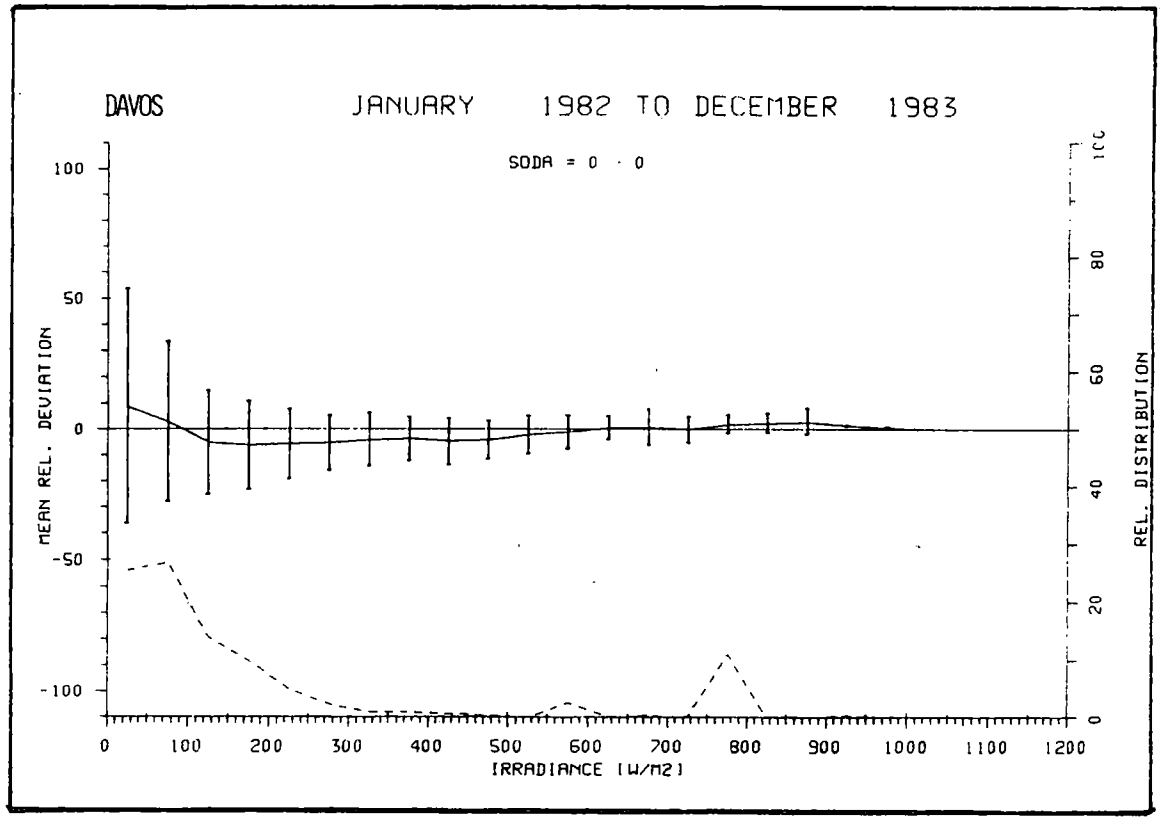

Fig. 4.16 Same as Fig. 4.15 for the no sun cases.

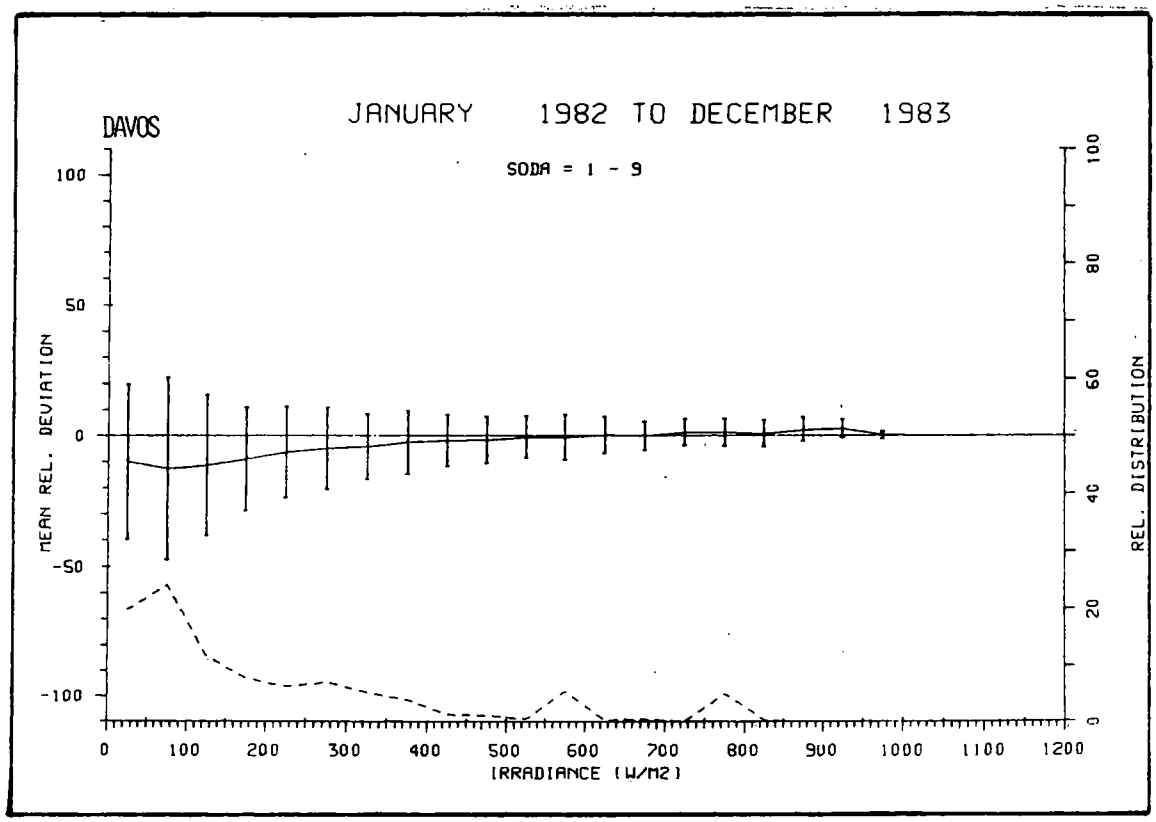

Fig. 4.17 Same as Fig. 4.15 for sunshine durations from 1 to 9 minutes.

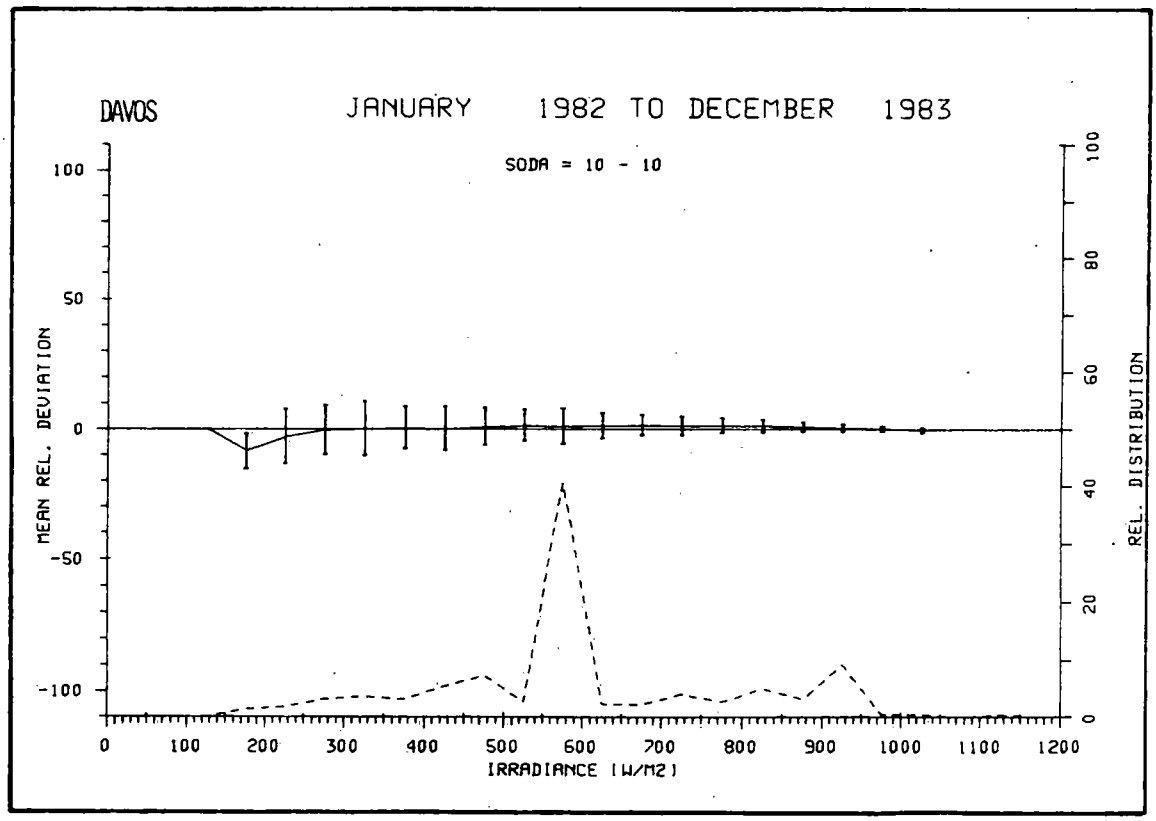

Fig. 4.18 Same as Fig. 4.15 for the full sun cases.

feel however that this finer procedure is not necessary since the pyranometers are known to show more than ± 2% uncertainty. A careful check of the scaling factor of the pyranometer should be performed before drawing any final conclusions about the quality of these results. Furthermore, the resolution of the data acquisition system is relatively broad for low intensities (10 W/m2), so that comparisons of hourly values should yield better results from this point of view.

4.3 Conclusion

The preceding results concerning the RASTA system confirm the conclusions of the previous work on that topic (1). The whole system has a very satisfactory behaviour and, as far as this study is concerned, is well suited for automatic networks. Teething problems are unavoidable for every new instruments, as illustrated in chapter 2. These difficulties yield however very important information for mass production of such instruments.

The investigated RASTA unit is a prototype and has to be considered as such. Any production should be started only when different modules of the electronic are improved, i.e. more adapted industry-compatible circuits and improved operational state flagging. This is of course dependant on the producer's state of technology and on the maintenance staff's possibilities and wishes.

Taking into account the preceding remarks, we strongly recommend the installation of more units within the ANETZ network in order to gather more thorough information about the radiative energy budget all over Switzerland. Eight new locations would cover broadly the different climatic regions of the country:

1. Locarno-Monti for the Tessin region,
2. St-Gallen for the East plateau,
3. Kloten for long term climatological needs,
4. Payerne for the West plateau and because of the experimental field facilities,
5. Lausanne for the Lemanic bassin climate,
6. Sion for Wallis climate,
7. La Chaux-de-Fonds for Jura,
8. Säntis or preferably Jungfraujoch for high alpine climate.

5. LUMINOSITY

As mentionned in the introduction, the "luxmeters" in operation on the ANETZ network are simple solar cells which have been extensively calibrated against a true digital luminosity recorder, yielding the following approximation formula:

$$I = 10^{**}((Im+245)/100) \quad [lux] \pm 25\%$$

where Im is the digitalized signal available from the network computer. A silicon diode has a maximum spectral response at about 850 nm, yielding a strong infrared sensitivity: this leads to overestimates of the intensities by red-coloured sunrises and sunsets. However, as the instruments show an approximately cosine square geometrical sensitivity, the two effects more or less compensate each other for low solar elevations. Another characteristic has to be underlined for the full understanding of the following study; the luminosity values are instantaneous measurements performed once every 10 minutes. They are therefore NOT integrated over the whole period as for the other units. This detail will have to be taken into account for comparisons with other instruments, but should not lead to critical difficulties as it will be significant only for rapidly varying cloud conditions.

The present section is divided in two main topics dealing with the diurnal and nightly behaviour of the recorded luminosity. For the diurnal information, the readings can be compared with the pyranometers' irradiances, though the spectral sensitivities of the two instruments are quite different. At night, such comparisons are impossible due to the lack of sensitivity of the pyranometers so that the investigation is restricted to the hypothetical use of this information for the determination of the cloud cover and a comparison with observations of the latter.

5.1 Diurnal behaviour

Direct comparisons between the luminosity and global irradiance values show a very good linear correlation between the two sets of measurements. However, there is an evident departure from linearity for small intensities of the global irradiance which can be explained by the low resolution of the data and the poor behaviour of the pyranometers for this kind of situation (section 3).

STATION : DAVOS					
Year	SODA	a	b	r^2	Nb. of points
1982	0-0	0.015	0.942	0.945	13990
1983	0-0	0.016	0.937	0.937	14238
1982	10-10	0.067	0.823	0.965	7921
1983	10-10	0.066	0.823	0.969	8171
1982	1-10	0.100	0.784	0.878	10988
1983	1-10	0.097	0.786	0.883	11047
1982	0-10	0.013	0.963	0.950	24978 } all data
1983	0-10	0.013	0.964	0.944	25285 }

Table 4.1. Results of the regressions performed between the global irradiance and the luminosity during the day following :

$$G_H = a * (I_{lux})^b$$

for two years and different sunshine duration classes (column SODA in minutes).

A power fit curve of the form

$$Gh = a\ (I_{lux})^b$$

is found to give the best results as displayed in table 4.1

The correlation coefficients may be considered as excellent. The best values are obtained by full sun (s = 10-10) and no-sun (s = 0-0) conditions while the broken cloud cover cases (S = 1-10) show some degradation which can be easily explained by the integral over 10 minutes of the pyranometer values and the instantaneous measurement of the luminosity.

Figures 5.1a to 5.1d show for 1982 the mean deviation between global irradiances measured by the pyranometer and computed with the regression coefficients a and b displayed in table 4.1. The results for the full-sun cases are very good above a threshold value of 200 W/m^2 which also corresponds to the limit found in section 3. They are also satisfying for the cases where at least some sun was recognised (s = 1-10), but, in the absence of sun, the situation is not

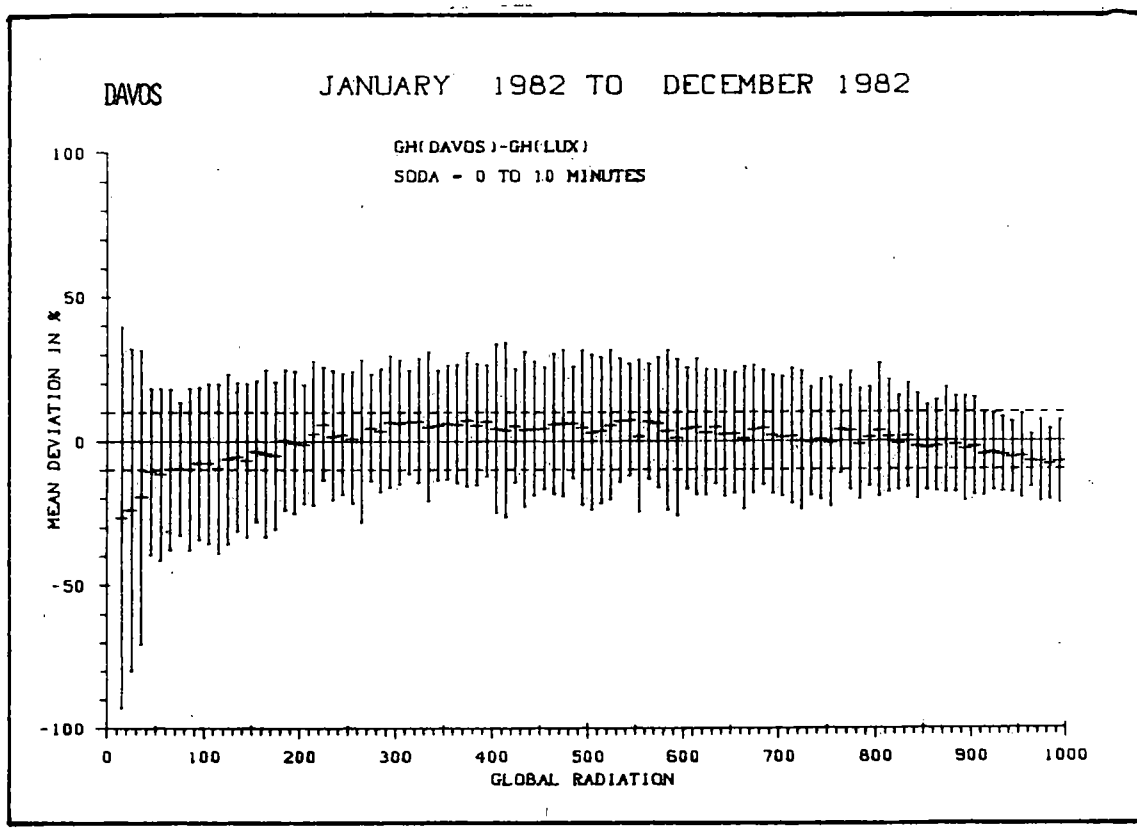

Fig. 5.1a Mean deviations between measured and computed global irradiances as function of the global measured irradiance for all sunshine durations. The vertical bars indicate the standard deviation of the mean.

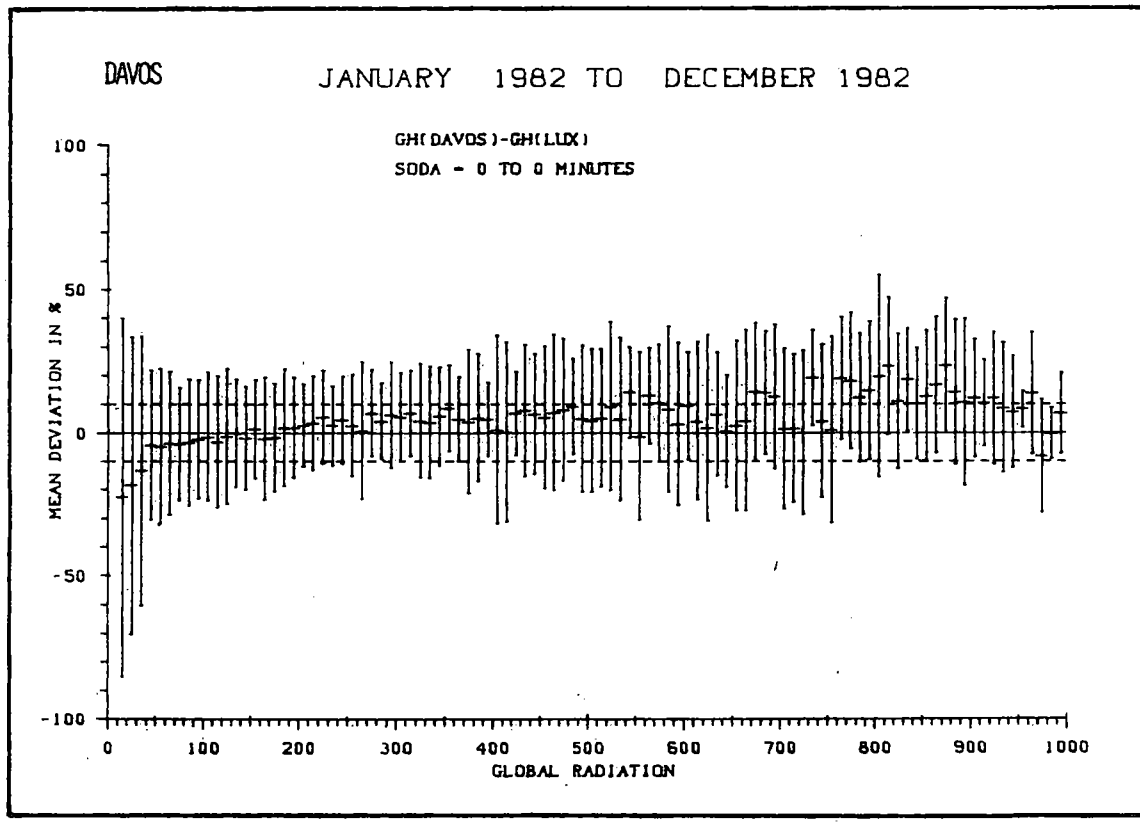

Fig. 5.1b Same as Fig 5.1a for the no sunshine cases.

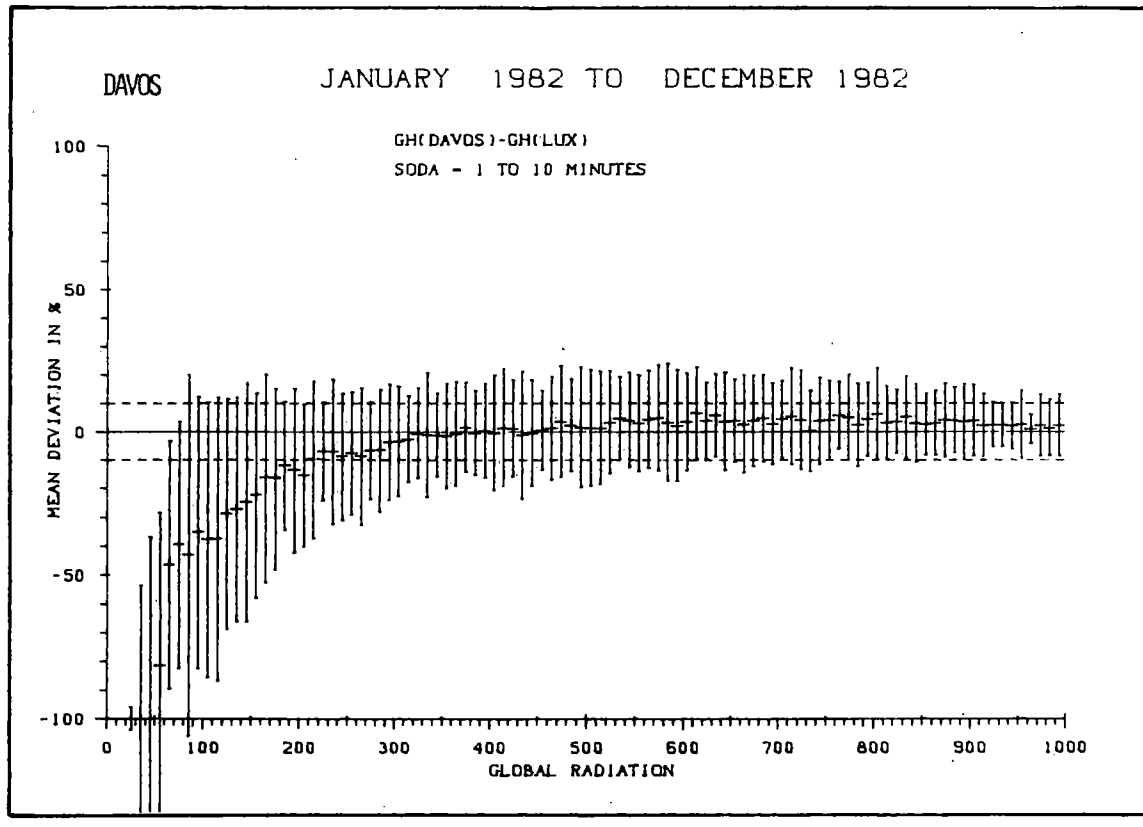

Fig. 5.1c Same as Fig. 5.1a for cases with at least 1 minute sunshine.

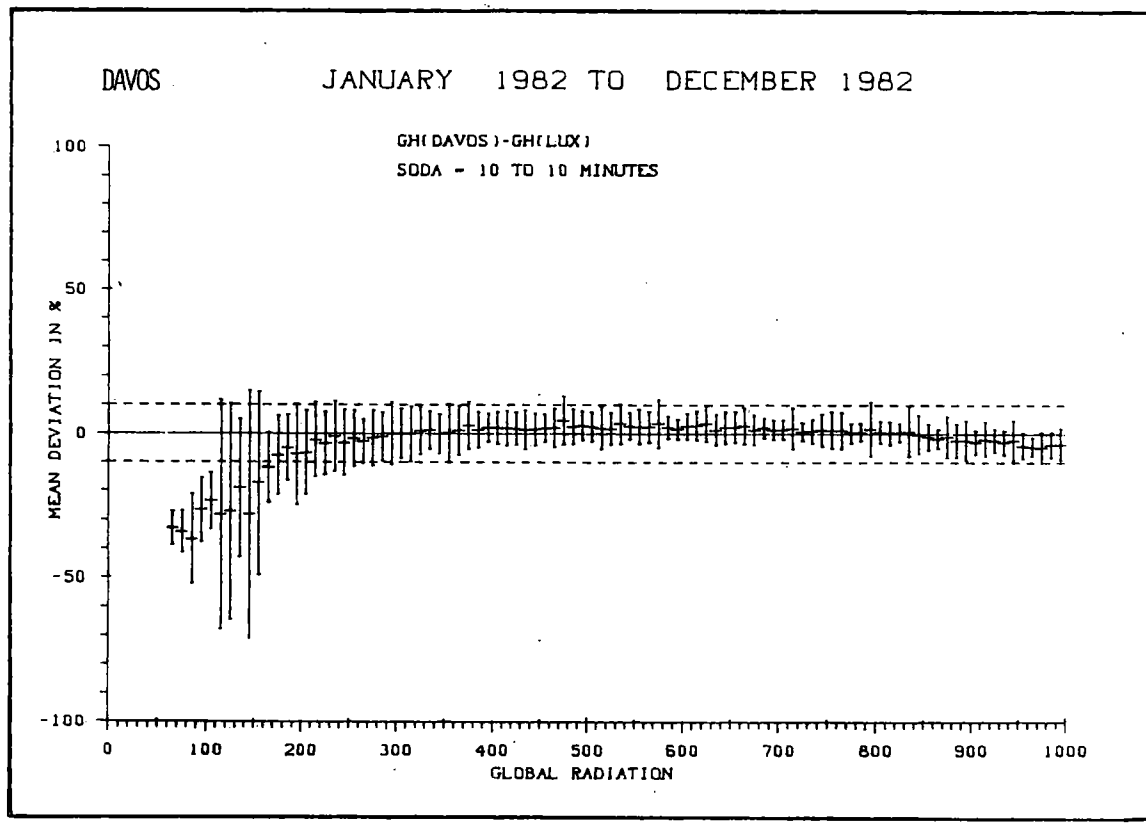

Fig. 5.1d Same as Fig. 5.1a for the full sunshine cases.

as convincing as for high intensities. This should however be handled with care because of the problems related to the sunshine recorder described in section 2. For the general case (figure 5.1a), the mean deviations remain within a range of ±10% for practically all intensities, with a reasonable accuracy for all situations, as shown by the standard deviation bars. A light curvature is noticeable in the middle intensity range leading to an underestimation of the computed values. This effect is probably related to either the spectral sensitivity of the diode or to the calibration method of the luxmeter. It should be kept in mind that the accuracy of the instrument is supposed to lie within a range of ±25%, thus impeding any better results.

Nevertheless, for the diurnal part of the day, the luminosity values may be well simulated from the global irradiances. It remains to be seen whether or not this behaviour is also true for the other stations of the network: this will be the scope of future work.

A further investigation can be performed in order to see if the above mentioned curvatures of the mean deviations are somehow dependant on the state of the sky, i.e. on the cloud cover. Figures 5.2a and 5.2b show the results of this attempt. The full lines refer to cases of positive deviations while the broken ones stand for the cases of negative deviations. The thin curves represent the relative number of cases for each cloud cover class (0/8, ..., 8/8). The medium curves show the relative number of cases from the total number of cases per cloud cover class. The thick curves represent the mean deviation per cloud cover class: in this case, the title of the ordinate is inadequate and the axis scale refers to the mean deviation in %.

The study of these results does not show any evident trend or possible correlation between the cloud cover and the mean deviations of the computed global radiation.

5.2 Luminosity at night

Two main light sources are at the root of the luminosity at night. The moon, whenever present, will play the role of the sun. This

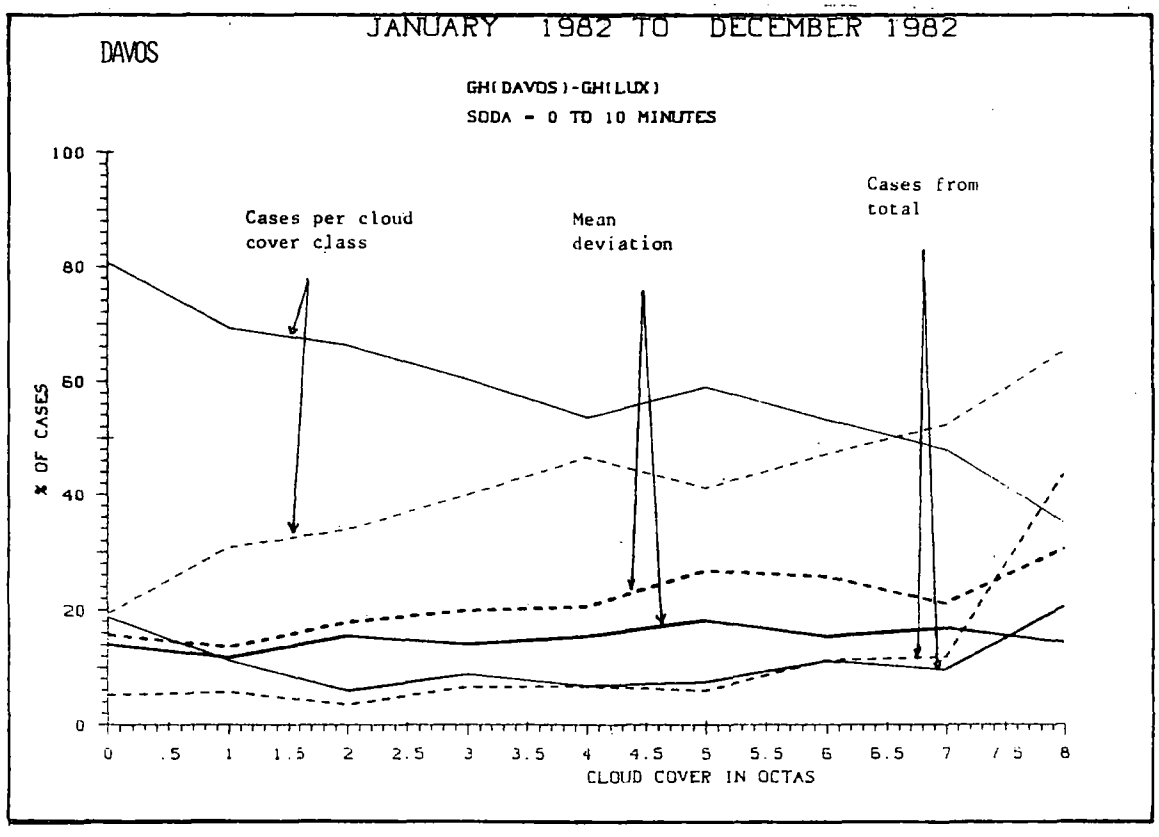

Fig. 5.2a Relative distribution of the deviations and of the mean deviations as a function of the observed cloud cover for year 1982. The full curves refer to positive deviations and the broken curves to negative deviations. For the mean deviations, the vertical axis represents the mean deviation in %.

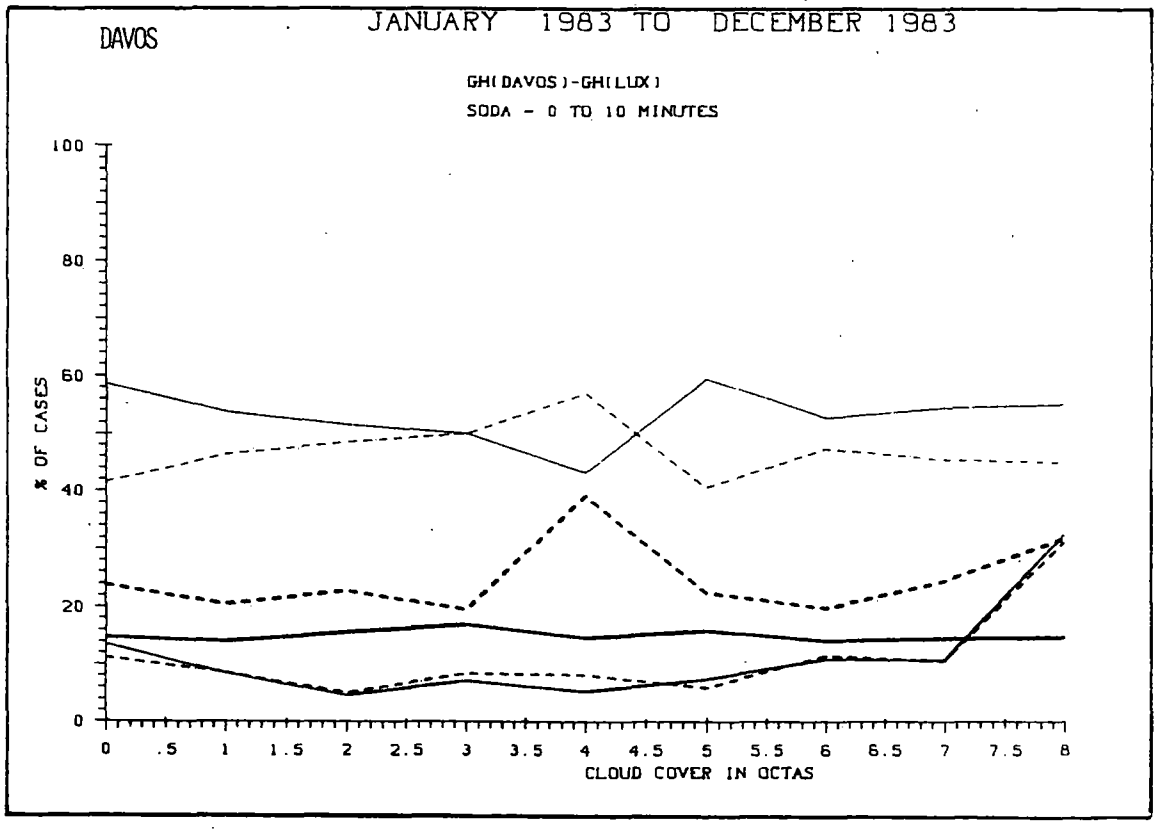

Fig. 5.2b. Same as Fig. 5.21 for year 1983.

means that the position and luminosity of the earth's satellite have to be computed, a task more complicated than for the sun. Artificial light sources, especially in the case of Davos, have also to be taken into account, whether the moon is shining or not. As very small intensities are involved at night, one can expect that the disturbances arising from man-made light sources will be a serious drawback for the evalution of the measurements since they are unpredictable and highly variable. For this purpose, a second station (Guetsch) has been chosen which is located at about 100 Km flight distance from Davos, completely remote in the mountains and, a very useful fact, a synoptic station with visual observations at a 3 hours frequency. This second station should be practically free of artificial interferences.

The moon elevation, azimuth, distance and phase are computed by the approximation trigonometric formulas presented in (3). Its luminosity at the mean moon-earth distance is taken from (4) and fits with other values found in the literature. The following formula is used as an approximation of the night luminosity:

$$I = IO \cdot \sin(h) \cdot p \cdot \exp(-T \cdot m) + 0.0018 \text{ (lux)}$$

where

I = moon luminosity on a horizontal surface,
IO = extraterrestrial value of the moon luminosity at mean sun-earth distance: IO = 0.311 lux ,
h = moon elevation,
p = moon phase,
T = atmospheric extinction: T = 0.1,
m = relative airmass.

An offset is added in order to take into account the residual luminosity of the sky (4). The whole procedure leads of course to a very rough approximation of the night luminosity.

The validity of the above simulation can be estimated by looking at figure 5.3 where the instantaneous measured luminosity at 0100 UT is plotted (full line) together with the computed moon luminosity at that time (broken line). For periods of bright moonlight, the matching is good, but for periods without moon, the approximation yields far too low intensities. This could be caused by the artifi-

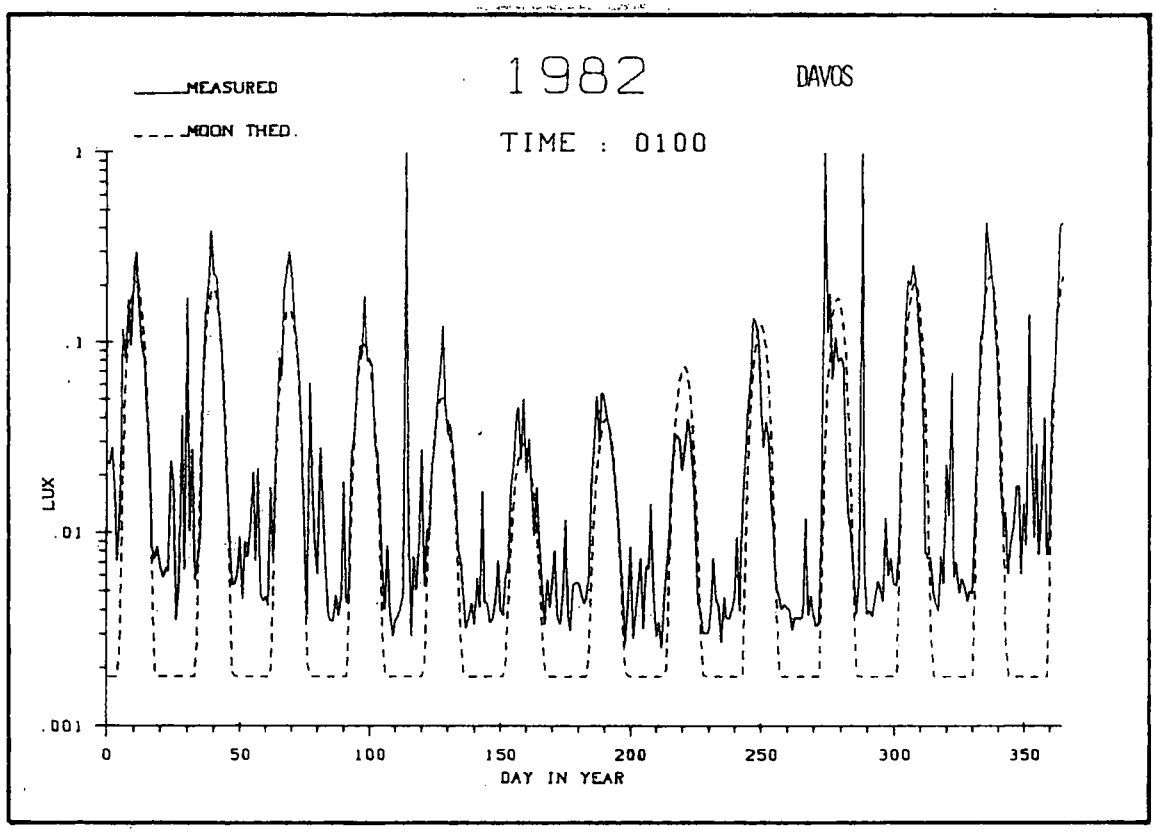

Fig. 5.3 Yearly variations of the luminosity at 0100 UT (full line) together with the simulated luminosity of the moon (broken curve). The peaks at 1 LUX represent missing data.

cial lights of the nearby town of Davos. Very high peaks are registered with magnitudes reaching more than 10 times the ground values. Also noticeable is the yearly mean trend of the values registered during the periods without moon. In order to wipe out short term artificial effects, the measured and simulated values are integrated between 0000 and 0100 UT in the following.

The study of a possible correlation between the behaviour of the measured luminosity and the cloud cover requires a more detailed representation, as shown on figures 5.4a and 5.4b for a winter and a summer month respectively. The lower diagram shows again the measured and estimated luminosities as a function of the day of the month. The upper part of the figures displays the cloud cover (NN: scale 0..8, full line) and the cloud opacity (ND: scale 0..5, broken line) for each day: since Davos is not a synoptic station, the mean of the preceding evening (1740 UT) and present morning (0640 UT) observations is taken as relevant information. This is of course a very coarse method. Figures 5.5a and 5.5b represent the same evaluation for the station Guetsch, though the cloud opacity is replaced

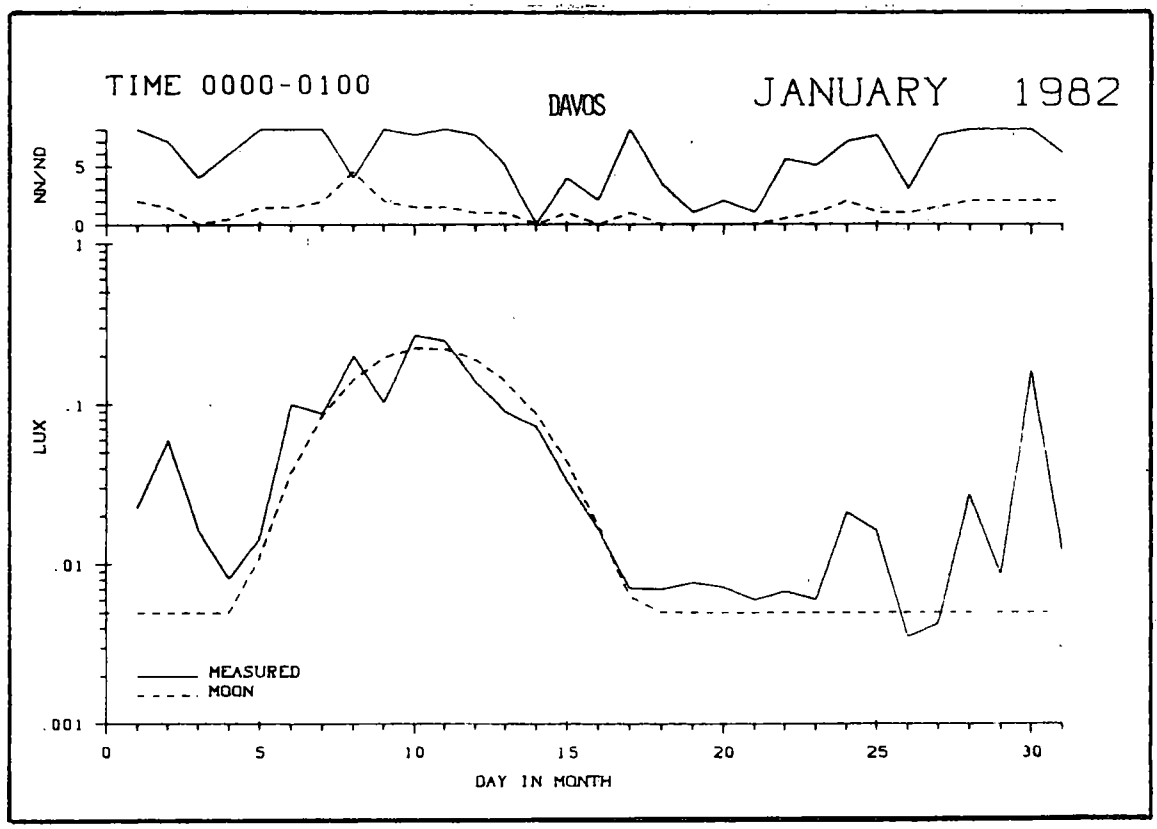

Fig. 5.4a Monthly variations of the recorded and simulated luminosity for a winter month. The upper diagram represents the cloud cover (NN) and the cloud opacity (ND) at the station (mean of evening and morning observations).
NN: scale 0..8, ND: scale 0..5
The luminosity values are integrated between 0000 UT and 0100 UT.

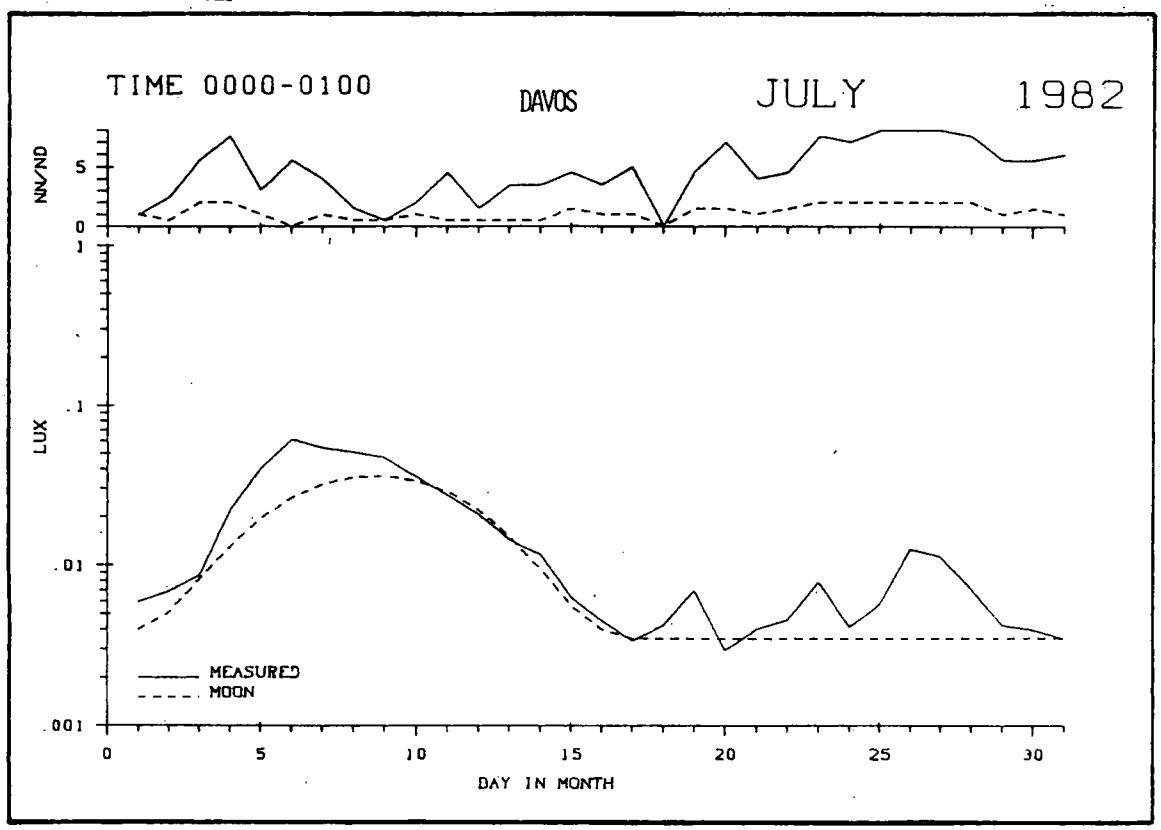

Fig. 5.4 b Same as Fig. 5.4a for a summer month.

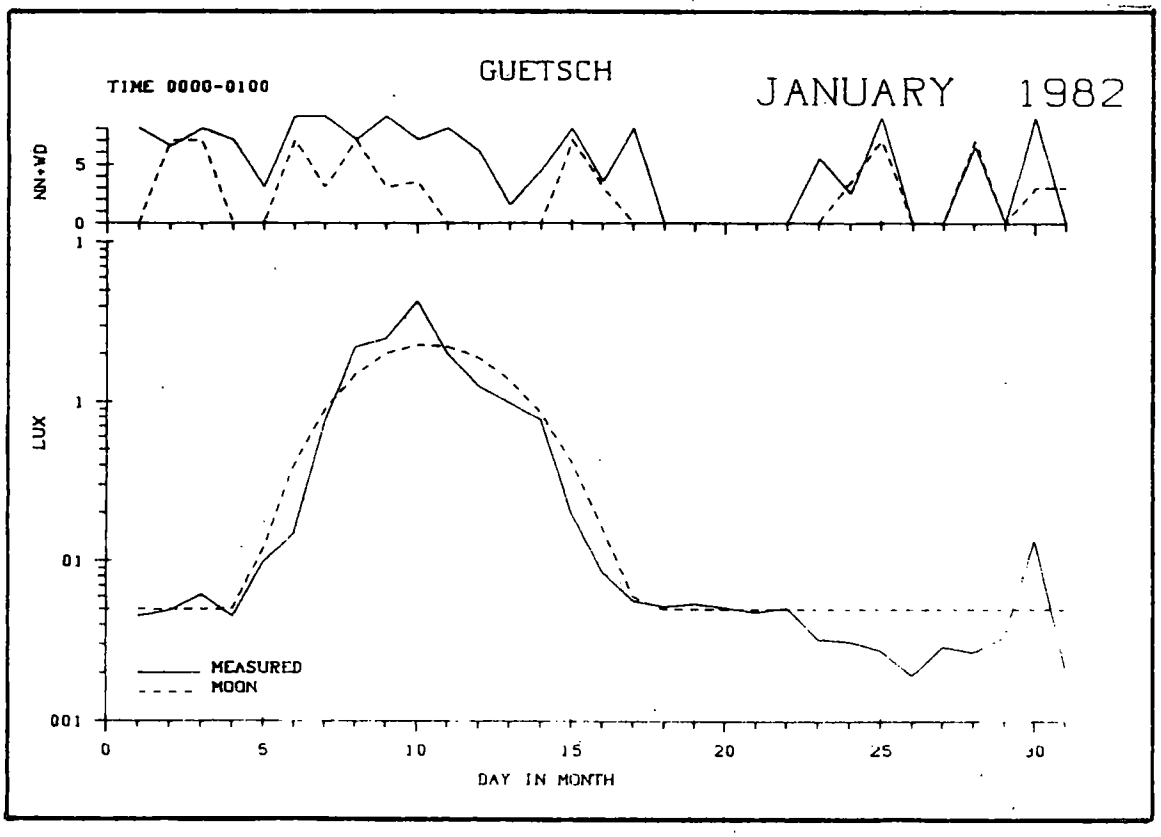

Fig. 5.5a Same as Fig. 5.4a for station Gütsch.

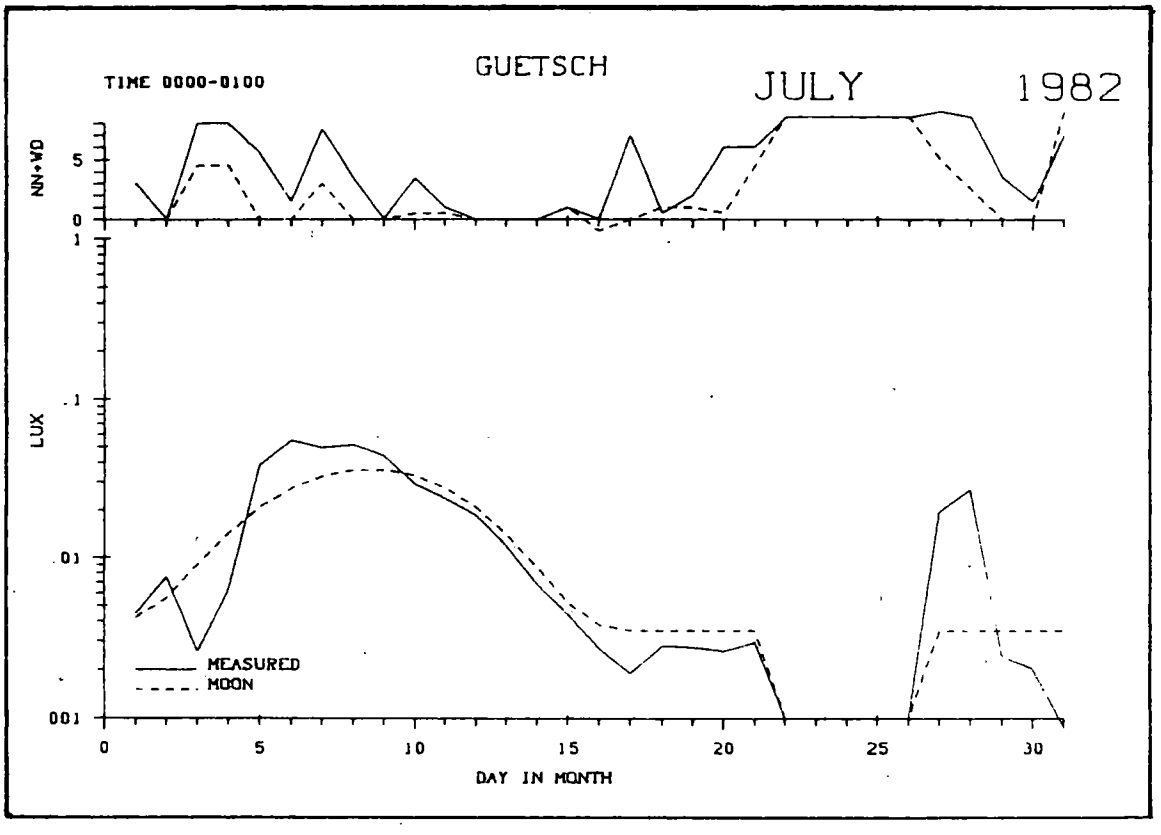

Fig. 5.5b Same as Fig. 5.4b for station Gütsch.

by the actual weather (WD : scale 0..9) estimation, since cloud opacity observations are not performed during the night. The residual luminosity is set to 0.005 lux for the winter months in order to take into account the reflexion by the snow and to 0,0035 lux for the summer months.

A detailed study of these figures does not show any obvious correlation between the variations of the measured luminosity and the cloud cover. This can be illustrated by plotting the deviations between the measured and simulated values of the luminosity against the cloud cover for both stations in cases of moonshine (moon >= 0.01 lux) and no moonshine (moon < 0,01 lux). The cloud opacity for Davos and the actual weather for Guetsch are marked on the plots (figures 5.6a to 5.6d).

This result was to be expected when comparing it to the behaviour of the global irradiance during the day. It is indeed rather illusory to attempt to determine the cloud cover only from the measurements of the global irradiance on a horizontal plane. This may be further illustrated by the following investigation. Since trained observers are stationed at the station Guetsch, the estimation of the cloud cover may be considered as good. It is therefore straightforward to study the behaviour of the recorded luminosity as function of the simulated luminosity for cloud covers 0/8 to 1/8 (figure 5.7a), 2/8 to 4/8 (figure 5.7b), 4/8 to 6/8 (figure 5.7c) and 6/8 to 8/8 (figure 5.7d). On these four diagrams, the residual luminosity is set to 0.0018 lux (4). It is evident that the global shape of the recorded luminosity remains the same independent of the cloud cover and is scattered around the 45 deg. line, which is actually a confirmation about the quality of the simulation. However, the scattering of the points is interesting, especially for the no-moon cases. Figure 5.8 shows for the cases without moonshine and for cloud cover less or equal to 1/8 the behaviour of the measured luminosity as function of the temperature. There is a slight tendency of decreased luminosity with rising temperatures. This result must be however carefully analysed since low temperatures occur in winter where snow reflection cannot be ignored and where the atmospheric transmission is usually higher than in summer (5). But a temperature dependance of the instrument can be expected since silicon diodes in the voltage mode have a -0.6%/K sensitivity change. Furthermore, the water vapour content of the atmosphere could play a significant role due to the spectral characteristics of the instrument.

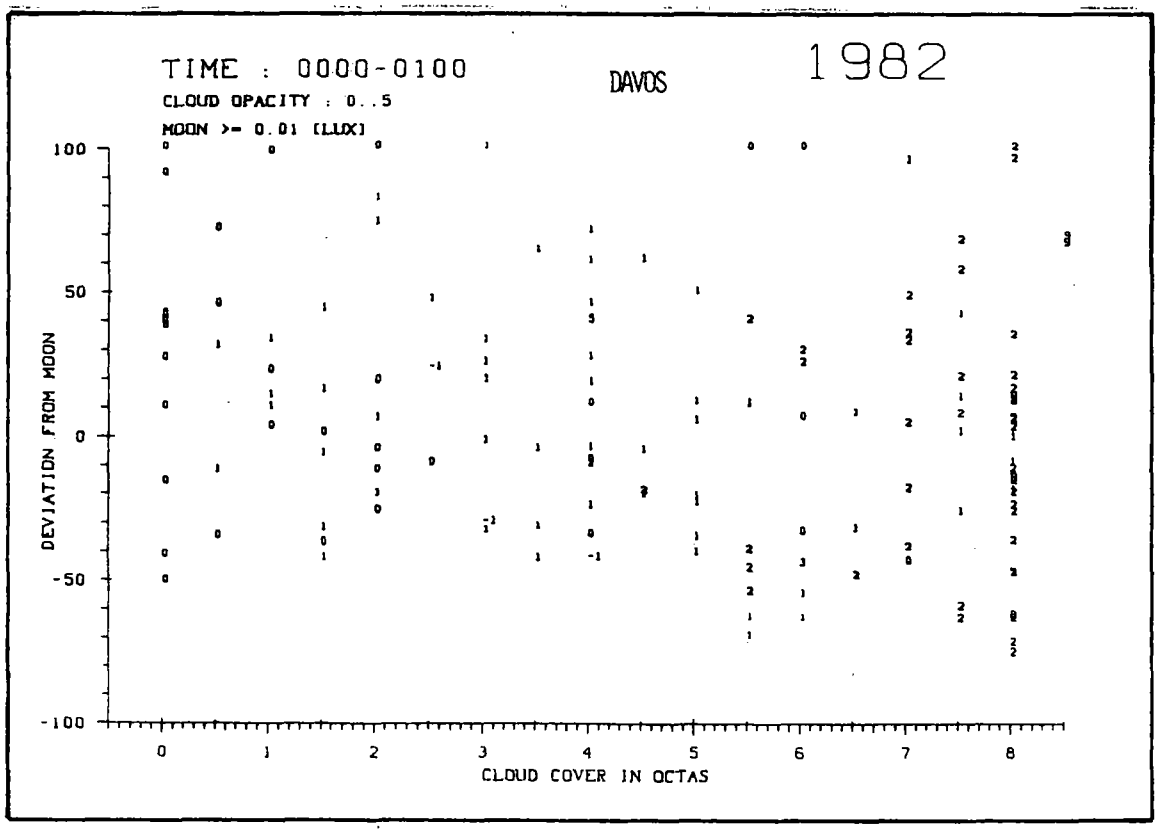

Fig. 5.6a Deviations between recorded and simulated luminosities as function of the cloud cover with moonshine (moon >= 0.01 Lux). The cloud opacity is marked on the plots.

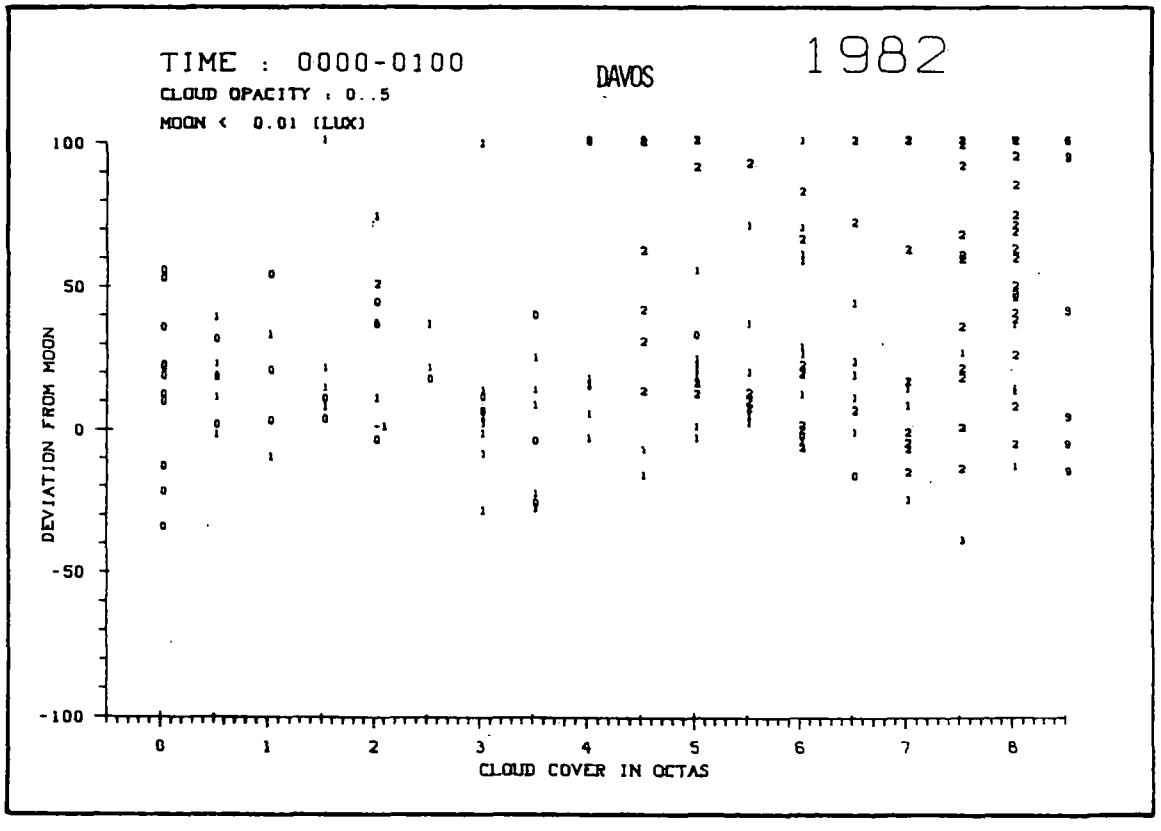

Fig. 5.6b Same as Fig. 5.6a for cases without moon (moon < 0.01 Lux).

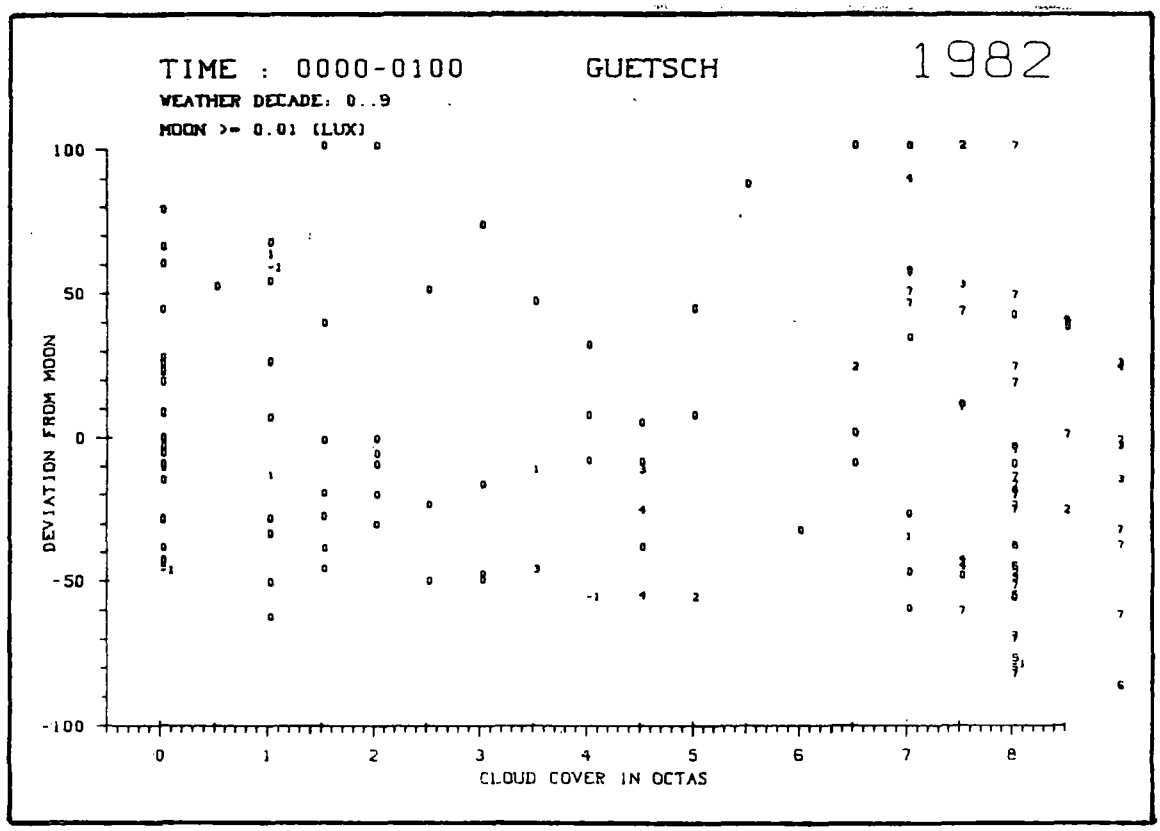

Fig. 5.6c Same as Fig. 5.6a for station Guetsch.

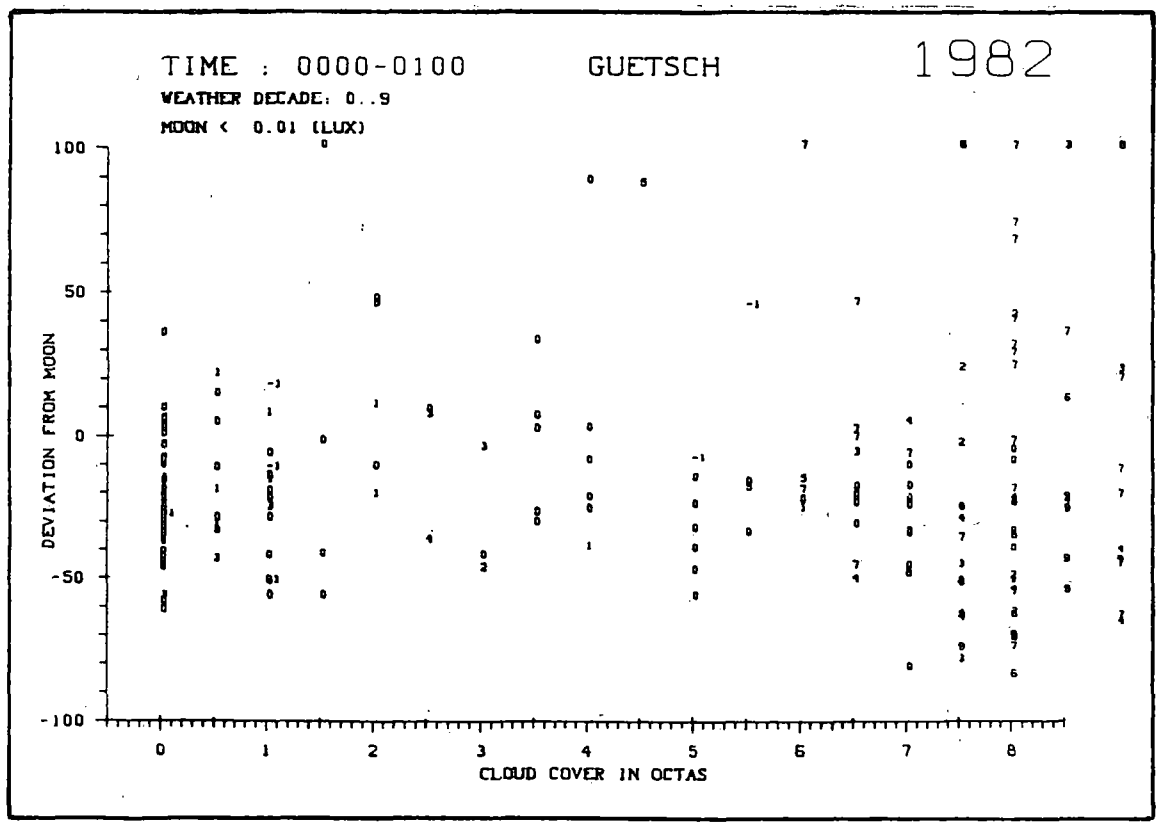

Fig. 5.6d Same as Fig. 5.6b for station Guetsch.

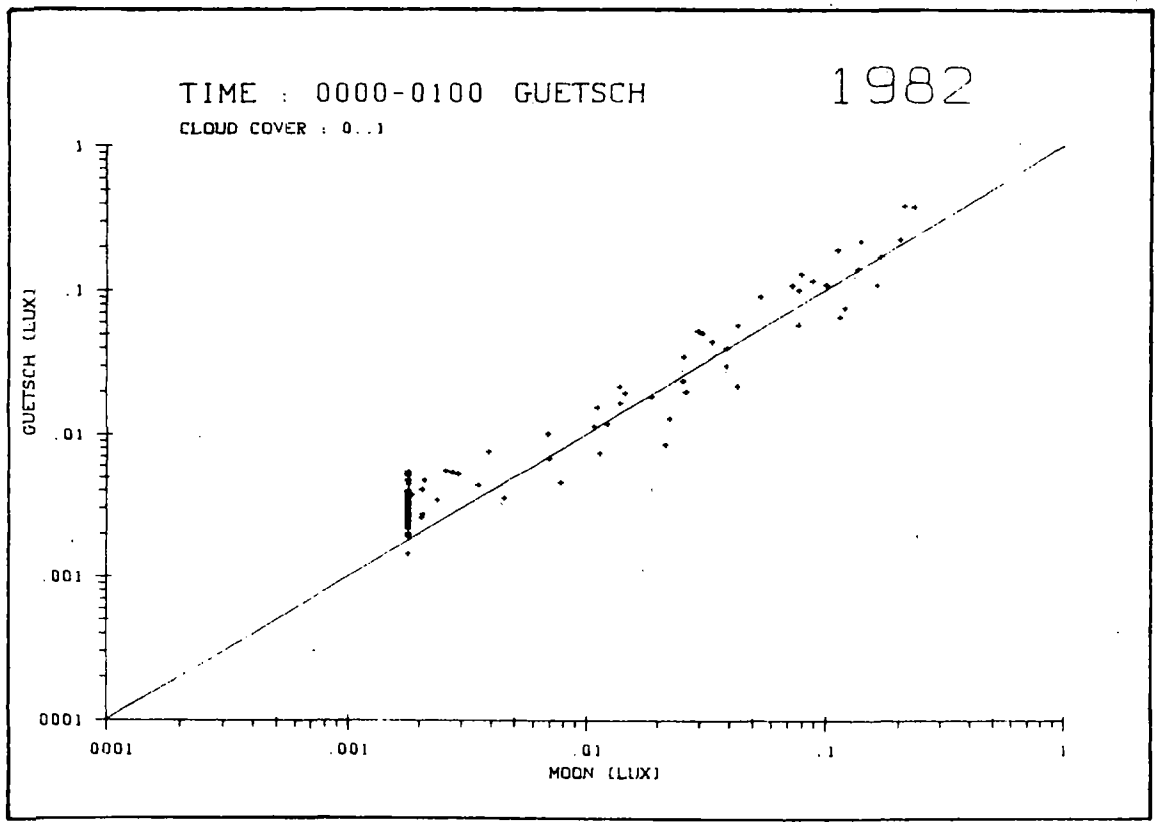

Fig. 5.7a Recorded luminosity at station Guetsch as function of the simulated moon intensity. The residual luminosity is set to 0.0018 Lux.
Cloud cover: 0/8 to 1/8

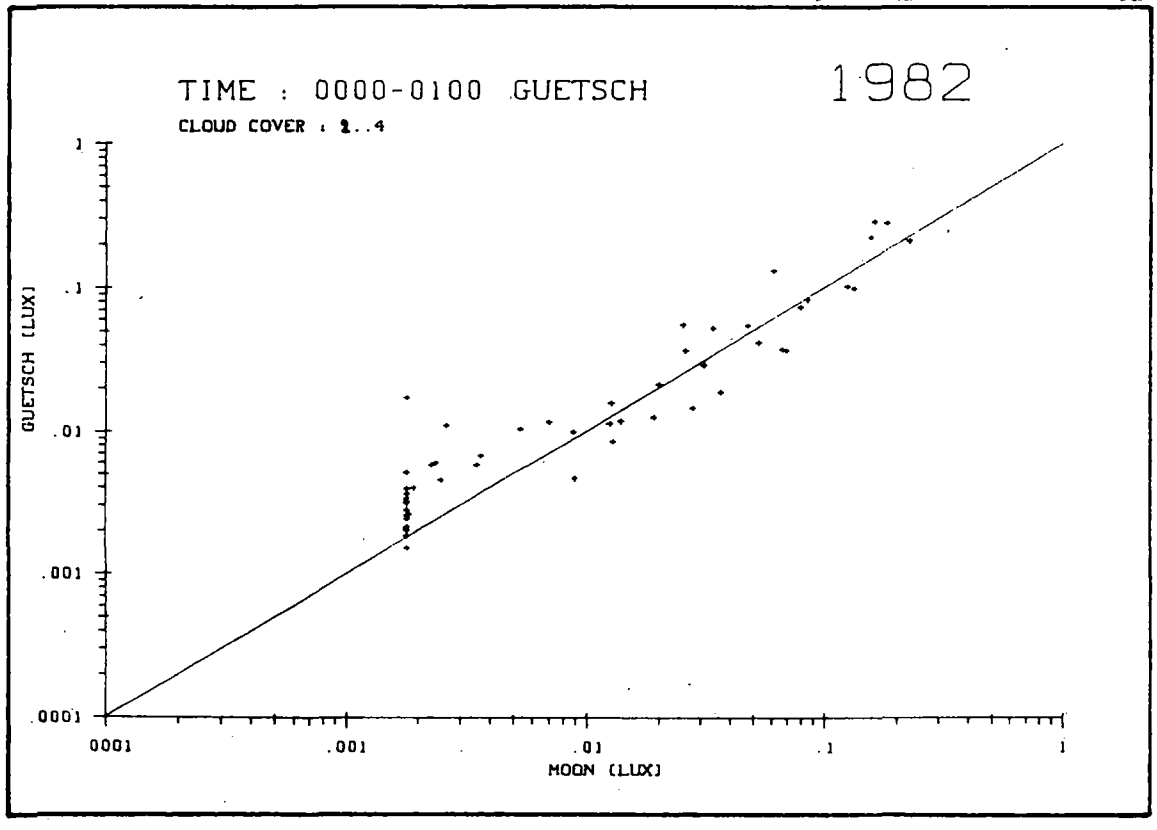

Fig. 5.7b Same as Fig. 5.7a for cloud cover 2/8 to 4/8.

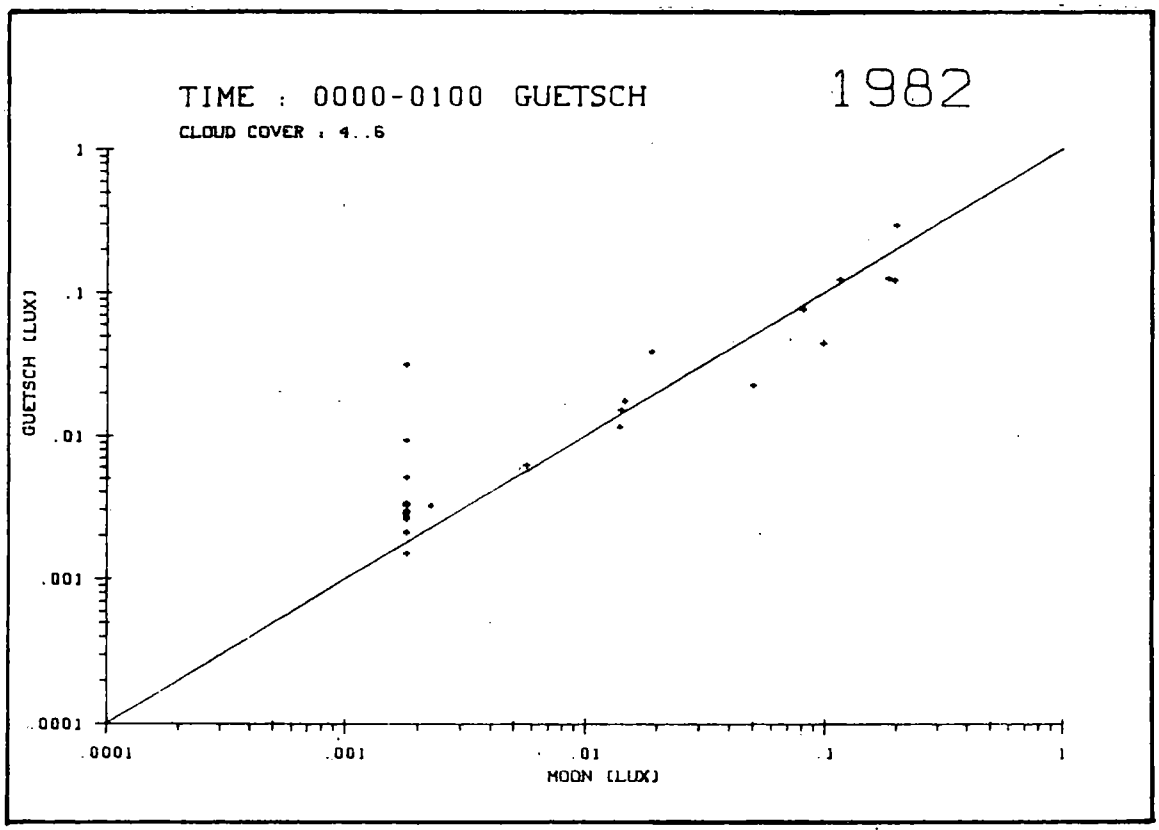

Fig. 5.7c Same as Fig. 5.7a for cloud cover 4/8 to 6/8.

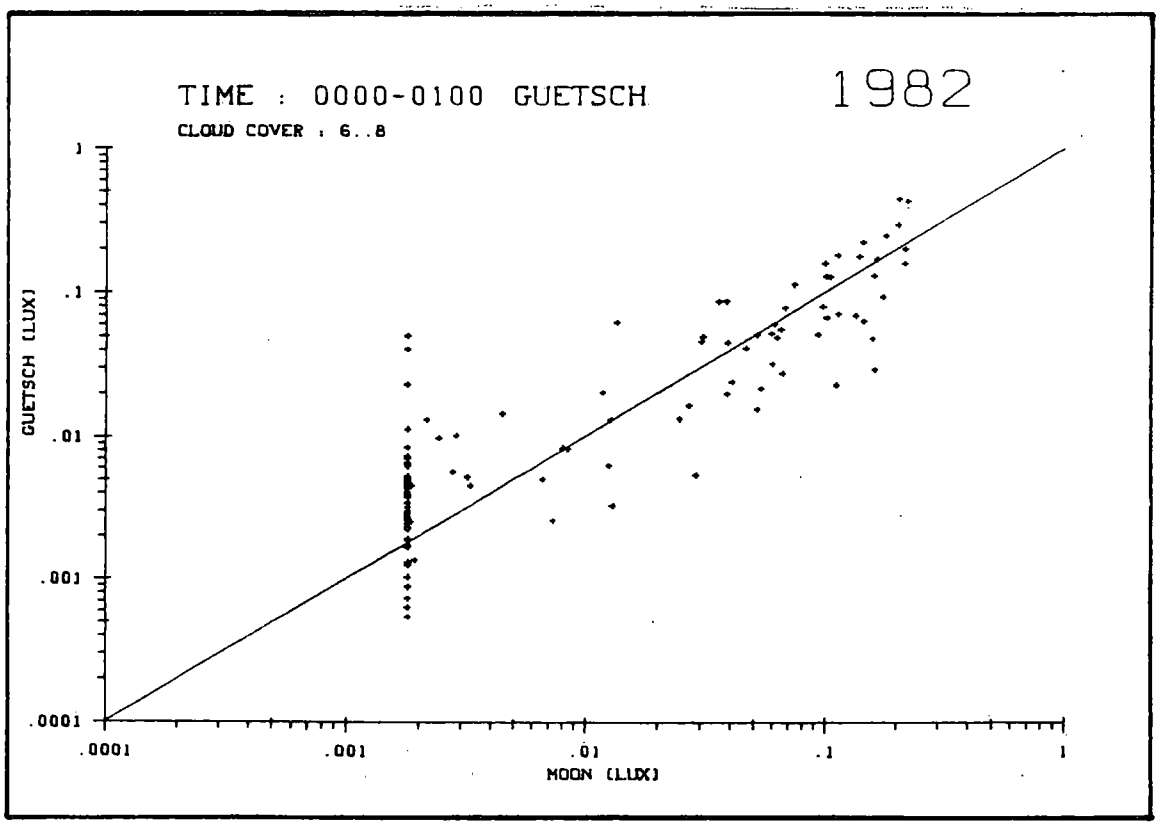

Fig. 5.7d Same as Fig. 5.7a for cloud cover 6/8 to 8/8.

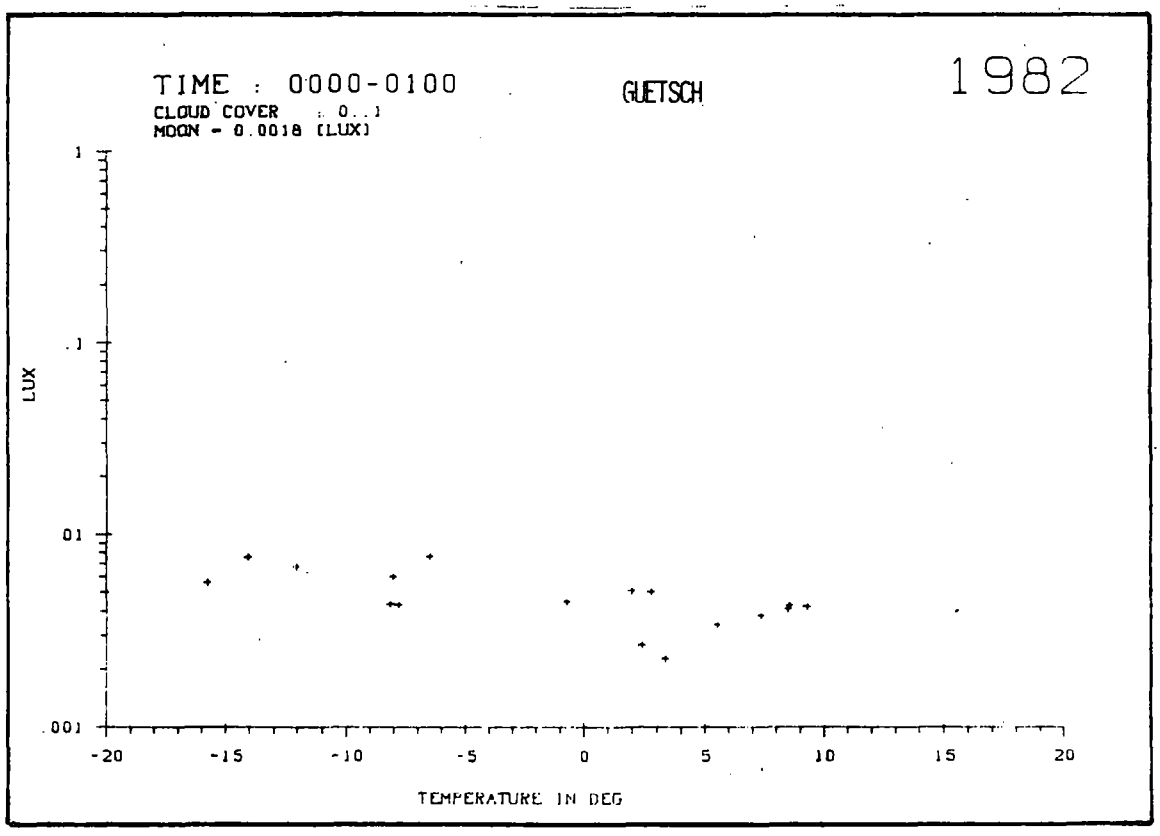

Fig. 5.8 Recorded luminosity as function of the temperature for cases without clouds (0/8 to 1/8) and without moonshine (moon intensity at residual value).

Since Davos and Guetsch are two stations which are not too far apart and are both mountain stations, it is possible to compare the simultaneous readings during moonshine (figure 5.9a) and without moon (figure 5.9b). More information can be gathered by plotting the deviations from the moon values: figure 5.10a shows that the deviation for both stations remain in a range of about ± 100% when the moon is shining. Figure 5.10b shows the same kind of results for the no-moon cases when taking into account the effect of the residual luminosity. The more important scattering of the points in the latter case is probably due to artificial lights. These last pictures are somehow puzzling: the synchronised deviations from the moon intensity for the two stations are pretty well correlated. Since the cloud cover dependence has to be rejected at least in the first order of approximation, some other parameter must be introduced. Therefore, a detailed analysis of the instruments' characteristics, like temperature and spectral dependence at very low intensities should be undertaken before any definitive conclusions are drawn.

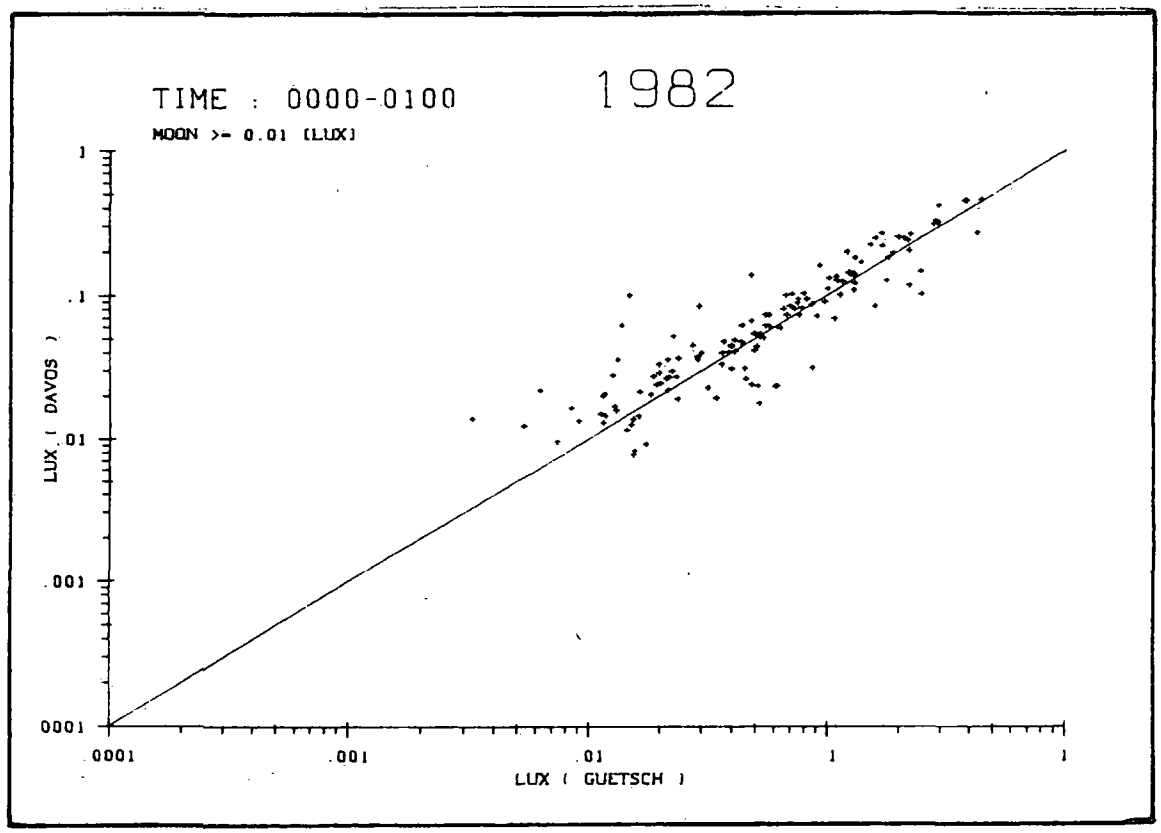

Fig. 5.9a Recorded luminosity at Davos as function of the recorded luminosity at Guetsch for cases with moonshine.

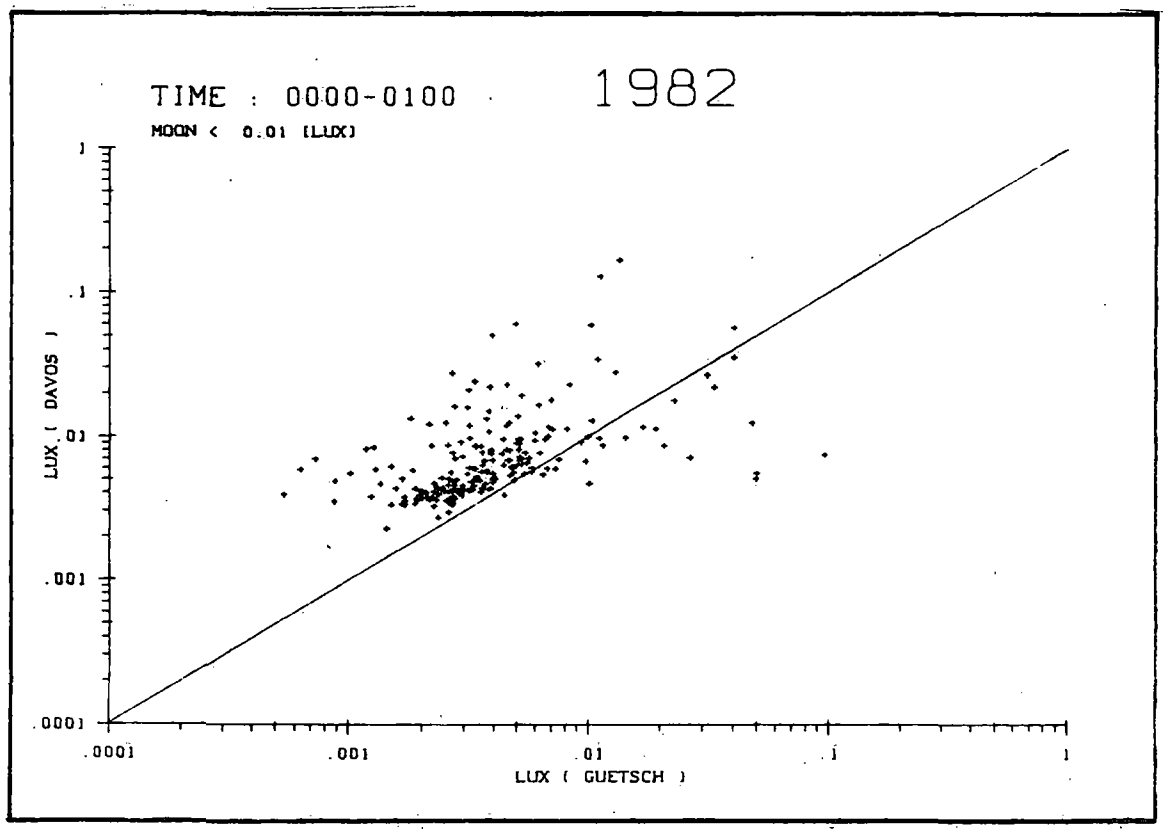

Fig. 5.9b Same as Fig. 5.9a for cases without moonshine.

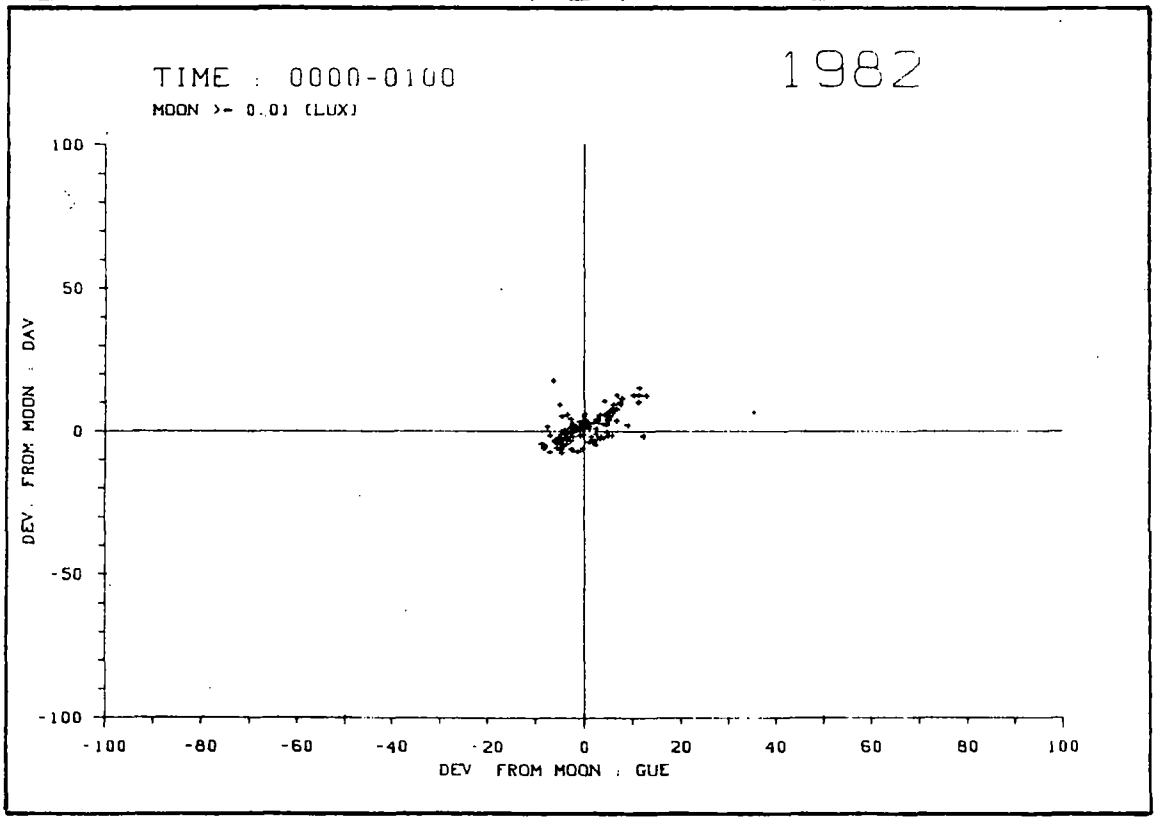

Fig. 5.10a Relative deviations of the recorded luminosity from the simulated luminosity at the two reference stations for cases with moonshine.
The numerical values of the axis have to be multiplied by 10 (20 = 200%)

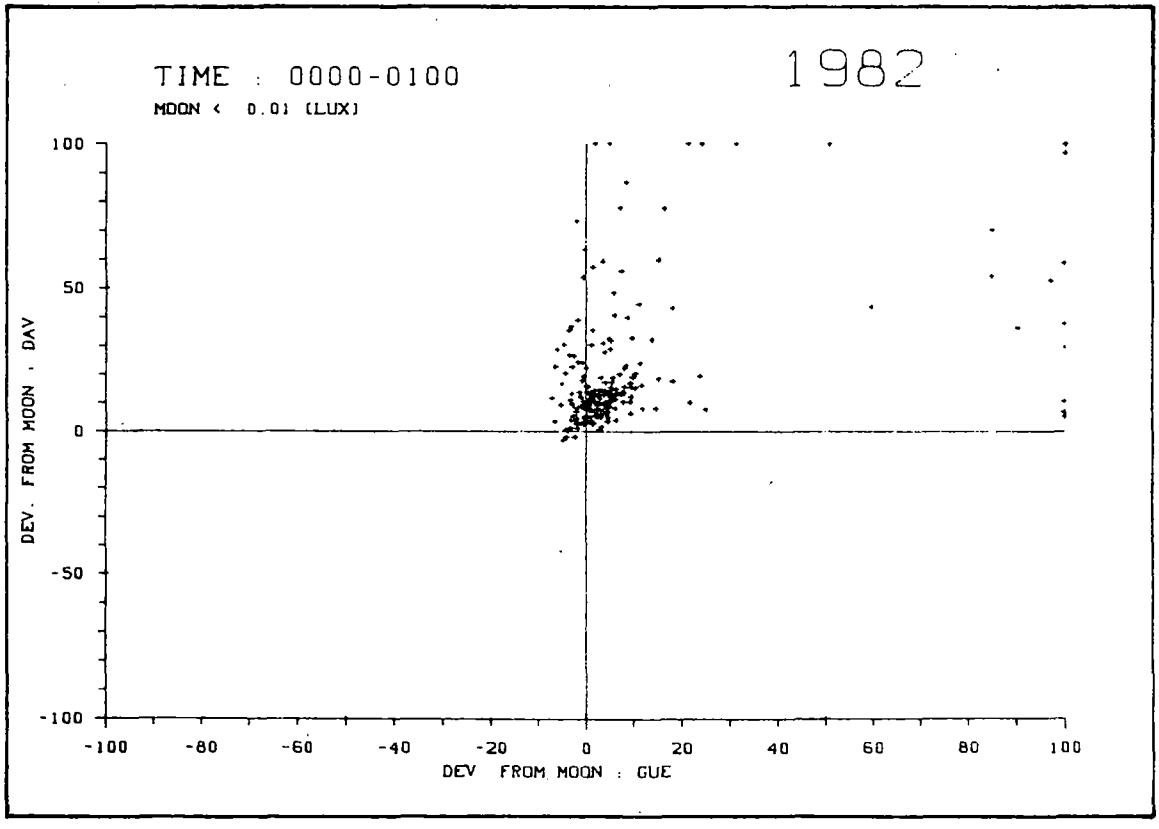

Fig. 5.10b Same as Fig. 5.10a for cases without moonshine.

The preceding investigations can now be summarized as follows:

- the night luminosity is highly dependent on the moon,
- the night luminosity is highly disturbed by the presence of artificial lights,
- no evident dependence on the cloud cover and opacity can be found
- temperature dependence of the instrument is significant,
- the instrument behaviour for the two investigated stations is well correlated.

Since the luxmeters in operation on the network are instruments integrating the radiation information over the whole upper hemisphere, their behaviour are not very different from those of the pyranometers, although the dynamic range of the diodes is about twice as large. When looking at all the efforts spent for the characterization of the pyranometers, at all the difficulties encountered and all the modeling attempts performed to simulate or make use of the global irradiance information, no obvious result can be expected from the measurements of the luminosity without an equivalent research investment: more specific indoor and outdoor tests have to be performed in order to understand the behaviour of these instruments operating in natural environment, before any further applications be undertaken.

6. CONCLUSIONS

The existence in Davos, Switzerland, of the World Radiation Center offers many possibilities to study the characteristics and behaviour of all kinds of radiation instruments and thus to develop control algorithms which can be subsequently applied to other less sophisticated stations.

The present work is an attempt to investigate the quality of the radiation sensors of the Swiss network ANETZ and of the new direct irradiance measurement automatic system RASTA. This is made possible by the redundancy of information available in Davos, such that a detailed knowledge of the intrinsic properties of the involved instruments may be collected.

The sunshine duration recorder has teehting problems which will be easily cured in the future.

The pyranometer results are satisfying beyond the threshold limit where the characteristics of the reference instrument allow accurate comparisons.

The luminosity values are strongly correlated with the global irradiance for the diurnal part of the day, but further investigations of their behaviour at night should be made.

The RASTA absolute radiometer did work properly over the test period: thus it is strongly recommended that a few other units be installed at appropriate locations in the country. The available information would then facilitate the computation of parameters not measured (e.g. diffuse radiation) and the development of quality control algorithms using:

- measured information: sunshine duration, direct and global horizontal irradiances,
- computed information: diffuse horizontal irradiance, atmospheric transmission,
- observations: weather, cloud cover,
- algorithms: definition of ranges, detection of errors, accurate modeling.

The gathered information potential would include, among others, the three components of the solar radiation, trends in atmospheric transmission, establishment of data bases for building industry and solar energy uses, etc....

Since RASTA includes a sun-tracker, it would be also advisable to add sunphotometers for spectral measurements yielding valuable information on the aerosol content and, at a few locations, on the background pollution. The ANETZ would then represent an extremely powerful tool for monitoring the radiative properties of the atmosphere.

Author's address:

Alain Heimo, Dr.sc.nat.
Swiss Meteorological Office
Krähbühlstrasse 58
CH-8044 Zürich

ACKNOWLEDGEMENTS:

Many thanks are due to Dr. C. Fröhlich, director of the WRCD, for his valuable advice and corrections of the manuscript.

Thanks are extended to Dr. A. Zelenka who helped to solve the spherical geometry problems concerning the RASTA sun-tracker alignment.

Neil Gregory from the EIR has kindly accepted to revise the English of the text.

REFERENCES

(1) Heimo, A.

Contrôle de qualité du système RASTA.
Swiss Meteorological Office, 1982 (unpublished).

(2) International Energy Agency

Results of an outdoor and indoor pyranometer comparison.
Task III, Document No. III. A.3, 1984.

(3) Nautical Almanac Office

Almanac for Computers 1978.
United Stated Naval Observatory, Washington, D.C. 20390.

(4) Bullrich, K.

Die Leuchtdichte des Himmels und die Globalbeleuchtungsstärke während der Dämmerung und in der Nacht.
Berichte des Deutsches Wetterdienstes in der US-Zone, nr. 4, Bad Kissingen (1948).

(5) Hoyt, D.V. and Fröhlich, C.

Atmospheric transmission at Davos, Switzerland, 1909-1979.
World Radiation Center, Davos, Switzerland, 1982.